# A PARTICULAR ROTATIONAL WAVE THEORY

By

CLAUDIO F. NEVES

A DISSERTATION PRESENTED TO THE GRADUATE SCHOOL
OF THE UNIVERSITY OF FLORIDA IN
PARTIAL FULFILLMENT OF THE REQUIREMENTS
FOR THE DEGREE OF DOCTOR OF PHILOSOPHY

UNIVERSITY OF FLORIDA

1987

# ACKNOWLEDGEMENTS

The author wishes to express his gratitude to Dr. Robert Dean, who has been for the past six years a source of motivation and support in pursuing this research program. His insight was always helpful in finding a physical interpretation for theoretical results derived in such an abstract topic as vorticity; however, his unbeatable optimism was equally important in overcoming difficulties.

Appreciation is extended to the committee members, Drs. Thomas Bowman, Joseph Hammack, James Kirby, and Hsiang Wang, who so much contributed towards the author's education.

Of particular value were the experiments conducted at the Coastal and Oceanographic Engineering Laboratory during the course of the graduate program, for which the author thanks the support given by Mr. Marc Perlin as well as the valuable craftsmanship and attention of Mr. Vernon Sparkman. Through Dr. Kirby, a special thank is conveyed to young Joshua, who donated one of his bath toys for the development of our understanding about vorticity.

An inseparable part of the academic program is the cooperation and exchange of ideas among fellow students, which serves as a continuation of the learning process in the classroom. With this in mind, the author extends his appreciation to colleagues and friends of the Department, especially to Kevin Bodge, William Dally, David Kriebel, Li-Hwa Lin, Sergio Schmidt, and Harley Winer.

After the gloomy hours in front of a computer terminal, when the evidence shows there is no life out of graduate school, the friendship of the author's roommates Elizabeth McCulloch, Eric Lessard, and Rick Copeland was greatly appreciated.

Finally, the author is grateful to his parents for their continuous encouragement during all these years.

During the first four years of the program, the author was granted a scholarship from the Brazilian research council (Conselho Nacional de Desenvolvimento Científico e Tecnológico), and during the last year an assitantship from the Coastal and Oceanographic Engineering Department, without which this study could not have been possible. In the last eighteen months, the author was granted a leave of absence from the Federal University of Rio de Janeiro, which is sincerely appreciated.

## TABLE OF CONTENTS

ACKNOWLEDGEMENTS . . . . . . . . . . . . . . . . . . . . . . . . ii

LIST OF FIGURES . . . . . . . . . . . . . . . . . . . . . . . . vi

LIST OF TABLES . . . . . . . . . . . . . . . . . . . . . . . . vii

LIST OF SYMBOLS . . . . . . . . . . . . . . . . . . . . . . . . ix

ABSTRACT . . . . . . . . . . . . . . . . . . . . . . . . xi

CHAPTERS

1 INTRODUCTION . . . . . . . . . . . . . . . . . . . . . . . . 1

2 REVIEW OF SOME ROTATIONAL WAVE THEORIES . . . . . . . . . 4

3 FORMULATION OF THE THEORY . . . . . . . . . . . . . . . . . . 12

  3.1 Mathematical Formulation . . . . . . . . . . . . . . . . . . 12

  3.2 Numerical Formulation . . . . . . . . . . . . . . . . . . 19

  3.3 Analytical Properties . . . . . . . . . . . . . . . . . . 21

  3.4 Derived Physical Quantities . . . . . . . . . . . . . . . . 24

    3.4.1 Vorticity Distribution . . . . . . . . . . . . . . . . 24

    3.4.2 Horizontal Velocity . . . . . . . . . . . . . . . . . 26

    3.4.3 Mean Horizontal Velocity . . . . . . . . . . . . . . . 27

    3.4.4 Free Surface Profile . . . . . . . . . . . . . . . . . 28

    3.4.5 Pressure . . . . . . . . . . . . . . . . . . . . . 28

4 NUMERICAL RESULTS . . . . . . . . . . . . . . . . . . . . . . 30

  4.1 Introduction . . . . . . . . . . . . . . . . . . . . . . . 30

  4.2 Influence of $\delta_1$ and $\delta_2$ . . . . . . . . . . . . . . . . . . . 32

  4.3 Numerical Relationship between the Parameters . . . . . . . . . . . 34

4.4 Horizontal Velocity Profile . . . . . . . . . . . . . . . . . . . . . . . . 34
4.5 Vorticity Distribution . . . . . . . . . . . . . . . . . . . . . . . . . . . 35
4.6 Free Surface Elevation and Wave Length . . . . . . . . . . . . . . . . 42
4.7 Pressure . . . . . . . . . . . . . . . . . . . . . . . . . . . . . . . . . . 45
5 SUMMARY OF RESULTS . . . . . . . . . . . . . . . . . . . . . . . . . 52
6 RECOMMENDATIONS . . . . . . . . . . . . . . . . . . . . . . . . . . . 54

APPENDICES

A SEPARABLE SOLUTIONS OF VORTICITY EQUATION . . . . . . . . . 56
B NUMERICAL COMPUTATION OF lcc- AND lsc- FUNCTIONS FROM PHASE PLANE TRAJECTORIES . . . . . . . . . . . . . . . . . . . 63
C MINIMIZATION PROCEDURE . . . . . . . . . . . . . . . . . . . . . . . 67
BIBLIOGRAPHY . . . . . . . . . . . . . . . . . . . . . . . . . . . . . . . . 69
BIOGRAPHICAL SKETCH . . . . . . . . . . . . . . . . . . . . . . . . . . 71

## LIST OF FIGURES

2.1 Transformation for Dubreil-Jacotin equation. . . . . . . . . . . . 6

3.1 Flow schematization. . . . . . . . . . . . . . . . . . . . . . . . 12

3.2 Function $lcc(y; \tilde{c}_2)$ . . . . . . . . . . . . . . . . . . . . . . 17

3.3 Function $lsc(y; \tilde{c}_2)$ . . . . . . . . . . . . . . . . . . . . . . 17

3.4 Phase plane trajectories . . . . . . . . . . . . . . . . . . . . . . 18

3.5 Vorticity distribution. . . . . . . . . . . . . . . . . . . . . . . . 25

3.6 Relative position of free surface elevation and horizontal velocity at the bottom. . . . . . . . . . . . . . . . . . . . . . . . . . . 27

3.7 Determination of $\eta$ . . . . . . . . . . . . . . . . . . . . . . . . 28

4.1 Mean quadratic error at the DFSBC. . . . . . . . . . . . . . . . . 33

4.2 Free surface elevation: Cases 1, 3, and 4. ( — ) SFWT, ( • ) present theory. . . . . . . . . . . . . . . . . . . . . . . . . . . . 46

4.3 Free surface elevation: Cases 2 and 2A. ( — ) SFWT, ( • ) present theory. . . . . . . . . . . . . . . . . . . . . . . . . . . . 47

4.4 Dimensionless dynamic pressure at the bottom: Case 2. . . . . . 48

A.1 Phase plane trajectories: Case B . . . . . . . . . . . . . . . . . . 59

A.2 Phase plane trajectories: Case C . . . . . . . . . . . . . . . . . . 61

# LIST OF TABLES

4.1 Wave parameters for cases studied. . . . . . . . . . . . . . . . . . 31

4.2 Theoretical parameters for cases studied. . . . . . . . . . . . . . 31

4.3 Validity of the solution. . . . . . . . . . . . . . . . . . . . . . . . . . 32

4.4 Present theory velocities at different elevations below trough level: Case 1. Values in m/sec. . . . . . . . . . . . . . . . . . . . . 36

4.5 SFWT velocities at different elevations below trough level: Case 1. Values in m/sec. . . . . . . . . . . . . . . . . . . . . . . . . . . 36

4.6 SFWT (1) velocities at different elevations below trough level: Case 1. Values in m/sec. . . . . . . . . . . . . . . . . . . . . . . . 36

4.7 Present theory velocities at different elevations below trough level: Case 2. Values in m/sec. . . . . . . . . . . . . . . . . . . . . 37

4.8 SFWT velocities at different elevations below trough level: Case 2. Values in m/sec. . . . . . . . . . . . . . . . . . . . . . . . . . . 37

4.9 SFWT (1) velocities at different elevations below trough level: Case 2. Values in m/sec. . . . . . . . . . . . . . . . . . . . . . . . 37

4.10 Present theory velocities at different elevations below trough level: Case 2A. Values in m/sec. . . . . . . . . . . . . . . . . . . . 38

4.11 SFWT velocities at different elevations below trough level: Case 2A. Values in m/sec. . . . . . . . . . . . . . . . . . . . . . . . . . 38

4.12 SFWT (1) velocities at different elevations below trough level: Case 2A. Values in m/sec. . . . . . . . . . . . . . . . . . . . . . . 38

4.13 Present theory velocities at different elevations below trough level: Case 3. Values in m/sec. . . . . . . . . . . . . . . . . . . . . 39

4.14 SFWT velocities at different elevations below trough level: Case 3. Values in m/sec. . . . . . . . . . . . . . . . . . . . . . . . . . . 39

4.15 SFWT (1) velocities at different elevations below trough level: Case 3. Values in m/sec. . . . . . . . . . . . . . . . . . . . . . . . 39

4.16 Present theory velocities at different elevations below trough level: Case 4. Values in m/sec. . . . . . . . . . . . . . . . . . . . . 40

4.17 SFWT velocities at different elevations below trough level: Case 4. Values in m/sec. . . . . . . . . . . . . . . . . . . . . . . . . . . 40

4.18 SFWT (1) velocities at different elevations below trough level: Case 4. Values in m/sec. . . . . . . . . . . . . . . . . . . . . . . . . 41

4.19 Wave length: comparison with Stream Function Theory ($L_{\mathrm{SF}}$), first order SFWT ($L_{\mathrm{I}}$), and Linear Wave Theory ($L_{\mathrm{L}}$). . . . . . . 43

4.20 Dimensionless vorticity under crest and trough: Case 1. . . . . . 43

4.21 Dimensionless vorticity under crest and trough: Case 2. . . . . . 43

4.22 Dimensionless vorticity under crest and trough: Case 2A. . . . . 44

4.23 Dimensionless vorticity under crest and trough: Case 3. . . . . . 44

4.24 Dimensionless vorticity under crest and trough: Case 4. . . . . . 44

4.25 Estimate of the wave motion contribution to the total vorticity. $\omega_0$ is the dimensionless value of vorticity used in the SFWT. . . 45

4.26 Dimensionless dynamic pressure distribution at crest and at trough: Case 1 . . . . . . . . . . . . . . . . . . . . . . . . . . . . . 49

4.27 Dimensionless dynamic pressure distribution at crest and at trough: Case 2 . . . . . . . . . . . . . . . . . . . . . . . . . . . . . 49

4.28 Dimensionless dynamic pressure distribution at crest and at trough: Case 2A . . . . . . . . . . . . . . . . . . . . . . . . . . . . 50

4.29 Dimensionless dynamic pressure distribution at crest and at trough: Case 3 . . . . . . . . . . . . . . . . . . . . . . . . . . . . . 50

4.30 Dimensionless dynamic pressure distribution at crest and at trough: Case 4 . . . . . . . . . . . . . . . . . . . . . . . . . . . . . 51

B.1 Computed parameters for $X(x;\gamma_2)$. . . . . . . . . . . . . . . . . 66

# LIST OF SYMBOLS

| | |
|---|---|
| $\hat{(\cdot)}$ | dimensional quantity |
| $(\,)\vert_c$ | value at wave crest |
| $(\,)\vert_t$ | value at wave trough |
| $A$ | constant of proportionality |
| $c$ | wave celerity |
| $f$ | arbitrary function for distribution of vorticity |
| $g$ | gravity acceleration |
| $h$ | water depth |
| $H$ | wave height |
| $k$ | wave number |
| $L$ | wave length |
| $p$ | total pressure |
| $P$ | dimensionless dynamic pressure |
| $s$ | elevation above the bottom |
| $T$ | wave period |
| $u$ | total horizontal velocity in moving reference frame |
| $u'$ | oscillatory component of horizontal velocity |
| $U$ | mean horizontal velocity (current) |
| $w$ | vertical velocity |
| $x$ | horizontal coordinate |
| $X$ | function of $x$ in the definition of the stream function |

| | |
|---|---|
| $X_n$ | coefficients for Stream Function Wave Theory |
| $z$ | vertical coordinate or elevation of streamline |
| $Z$ | function of $z$ in the definition of the stream function |
| $\alpha$ | ratio wave height to water depth |
| $\gamma_2$ | parameter for present theory |
| $\delta_1$ | parameter for present theory |
| $\delta_2$ | parameter for present theory |
| $\epsilon$ | wave number times depth |
| $\eta$ | free surface elevation |
| $\phi$ | arbitrary function |
| $\psi$ | stream function |
| $\psi_\eta$ | value of the stream function at the free surface |
| $\omega$ | vorticity |

Abstract of Dissertation Presented to the Graduate School
of the University of Florida in Partial Fulfillment of the
Requirements for the Degree of Doctor of Philosophy

# A PARTICULAR ROTATIONAL WAVE THEORY

By

CLAUDIO F. NEVES

December 1987

Chairman: Dr. Robert G. Dean
Major Department: Engineering Sciences

A formal solution of the Euler equations of motion is derived analytically using the method of separation of variables on the two dimensional vorticity equation. Physically, the solution corresponds to waves propagating on a current which has a vorticity distribution expressed as $\psi \log \psi$, where $\psi$ is the stream function. The kinematic free surface boundary condition is satisfied exactly, while the dynamic free surface boundary condition is satisfied in the root mean square sense by an iterative procedure.

The results are compared with the stream function solution for waves on a current of uniform shear as developed elsewhere in the literature.

# CHAPTER 1
# INTRODUCTION

One of the most common assumptions in wave dynamics with regard to applications in coastal engineering is the absence of vorticity. Stokes was the first to make use of this hypothesis, which can be justified both by theoretical considerations and by experimental verification. The problem of water waves, in spite of its complexity, is very much simplified if the motion is irrotational, since it can be reduced to the determination of a scalar quantity, the velocity potential.

In a more general approach, however, the problem can also be cast in terms of the stream function. As a matter of fact, the velocity potential and the stream function turn out to be complex conjugate functions, which allows the use of conformal mapping and other techniques in complex analysis for obtaining the solution. In the presence of vorticity, it is no longer possible to define the velocity potential but there still exists a stream function.

Although beyond the scope of the present work, in the general case of three dimensional flows of an incompressible fluid, it is always possible to define a vector potential, or vector stream function, as Helmholtz (1858) has proven. The vorticity, defined as the curl of the velocity field, is obtained as minus the Laplacian of that vector potential. The stream function usually presented for two dimensional flows is just one component of the Helmholtz potential, the others being identically zero.

The theory being presently formulated is valid for two dimensional, rotational flows, periodic in space and time, and corresponding to waves of permanent form propagating on a current with a particular vertical profile. Viscosity is neglected and the water depth is uniform. Upon the introduction of a Gallilean transformation of coordinates following the waves, the motion becomes steady in this moving reference frame and the basic governing equation, the conservation of vorticity, is solved by the method of separation of variables. Inside the fluid domain the solution is exact and the boundary conditions are then approximately satisfied using a numerical procedure similar to the one developed by Dean (1965) and Dalrymple (1973).

The justification for studying rotational wave theories in inviscid fluids may not be so evident. First, with some reason, one might argue that the irrotational theories give very good results. Second, the source of vorticity may be questionable in the absence of viscosity, since intuitively these two concepts are much linked: however, because vorticity is a property of the flow instead of being one of the fluid, those concepts are independent. Actually, it is possible to obtain irrotational flows of viscous fluids as well as rotational flows of inviscid fluids. Vorticity is intrinsically related to the inertia forces, and viscosity only causes vorticity to be diffused, usually from the boundaries. Therefore, there is nothing in the Euler equations of motion which may "a priori" rule out the existence of vorticity. Further, in the absence of any physical mechanism of dissipation, it is possible that parts of the fluid be subject to rotational flows, yet immersed in a general potential flow.

Many applications require the determination of the wave characteristics in the presence of a non-uniform current, in which case neither the assumption of irrotationality nor the linear superposition of both flows may be valid. In this case, vorticity might be used as a way to model a turbulent current, and yet the large scale motion could still be governed by the Euler equations of motion. However, very few rotational wave theories have been developed for inviscid fluids. A review of previous theoretical research is presented in Chapter 2. Recently, with the development of laser anemometers, it has become feasible to indirectly measure vorticity, although work in this area is mainly concerned with breaking waves and therefore cannot be used as an experimental verification.

The theoretical formulation and the numerical method of solution are discussed in Chapter 3. Also, a qualitative description of derived quantities of practical interest — including the velocity profile, the vorticity distribution, the pressure field, among others — is included. In Chapter 4, the results of the present work are compared with those obtained from the stream function theory developed by Dalrymple (1973) for a linear shear current.

The general problem of waves riding on an arbitrary current remains unsolved, and essentially is equivalent to finding a general periodic solution of Euler's equation of motion. The present work is just an investigation of a particular solution and the numerical evidence of its existence. Nevertheless, it calls attention to two facts. First, for practical purposes, neglecting the existence of the current — or its vertical structure — may induce distortions, for instance, in the estimate of wave heights from pressure transducers or in the evaluation of forces induced on submerged bodies. Second, from the theoretical point of view, it is always possible to derive a three dimensional rotational flow knowing a two dimensional solution. Consider three orthogonal planes, such that a stream function is known on each plane. The vector potential formed with each of these functions as a component in the normal direction of the corresponding plane will be an admissible solution of Euler's equation in three dimensions. This is basically the same construction demonstrated by Yih (1955) for potential flows.

# CHAPTER 2
# REVIEW OF SOME ROTATIONAL WAVE THEORIES

The interaction between waves and a current with an arbitrary velocity profile is the natural motivation for the study of rotational wave theories. However, due to mathematical difficulties as well as lack of experimental verification, the topic has not been studied extensively. Recently, the interest in flows with vorticity has increased due to theoretical developments in understanding global properties of nonlinear partial differential equations, development of new numerical techniques, and also the use of more sophisticated equipment — both computers and laboratory devices. With respect to coastal engineering, a better understanding of waves in the presence of rotational flows would certainly be of practical interest. Peregrine (1976) presents a comprehensive overview of the subject of wave-current interaction and, for a more recent and updated review including major applications in coastal engineering, the reader should refer to Peregrine and Jonsson (1983) and Peregrine, Jonsson, and Galvin (1983).

According to Lamb (1932), probably the first theory to describe a wave motion in water of infinite depth was given by Gerstner in 1802. His theory was an exact solution of the equations of motion in Lagrangian coordinates, but the presence of vorticity was against the physical evidence, in favor of irrotational flow. The particles move in circular paths whose diameters decrease with depth, and the free surface has the shape of a trochoid. The vorticity,

$$\omega = -\frac{2\sigma(ka)^2 e^{2kz_0}}{1 - (ka)^2 e^{2kz_0}}$$

where $a$ is the wave amplitude and $z_0$ the mean vertical elevation of the particle, is maximum at the free surface and decreases exponentially. It is always negative, which means it is in the opposite direction of the orbital motion of the particles. This fact calls attention to an important property of vorticity: it can not be obtained from the observation of the trajectory of one single particle, but rather how this trajectory is traversed. Kinsman (1984) presents a derivation of the theory and points out that, because Gerstner's solutions are linear solutions of the Lagrangian equations of motion, they can be superposed.

Because of the difficulty in generating such a motion from the state of rest, and also because the irrotational hypothesis allowed the introduction of the complex velocity potential, which to some extent simplified the mathematical formulation of the problem of water waves, Gerstner's theory as well as other rotational theories have not been used.

Even for irrotational waves, there is no theory completely analytical theory which is uniformly valid from deep to shallow water. In the presence of a current the distinction in terms of water depth is more significant. For deep water waves, if one considers the simplest case of vorticity, a linear shear current, the velocity will grow without bounds with depth. Since this is not reasonable, it becomes necessary to model the current profile with some degree of discontinuity or nonuniformity. As a consequence, from the theoretical point of view, there will be different approaches depending on the depth of water: in one extreme, waves riding for instance on wind driven currents, in the other, waves propagating into estuaries.

Dubreil-Jacotin (1934) considered the general problem of waves with an arbitrary distribution of vorticity, and proved the existence of solution both for finite and infinite depth. Using the formulation of vorticity in terms of the stream function $\hat{\psi}$, she introduced a transformation of variables such that the elevation of the streamline, $\hat{z}$, became the independent variable. Therefore, instead of the usual

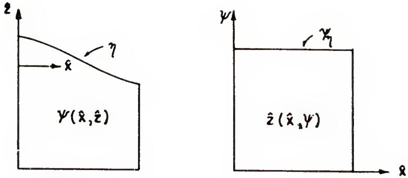

Figure 2.1: Transformation for Dubreil-Jacotin equation.

equation

$$\nabla^2\hat{\psi} = \hat{\psi}_{\hat{x}\hat{x}} + \hat{\psi}_{\hat{z}\hat{z}} = f(\hat{\psi}), \tag{2.1}$$

where the velocity field is obtained as

$$\hat{u} = -\hat{\psi}_{\hat{z}} \quad \text{and} \quad \hat{w} = \hat{\psi}_{\hat{x}},$$

by means of the transformation

$$\hat{\psi}(\hat{x},\hat{z}) \rightarrow \hat{z}(\hat{x},\hat{\psi})$$

the vorticity equation finally becomes

$$\left(1 + \hat{z}_{\hat{x}}^2\right)\hat{z}_{\hat{\psi}\hat{\psi}} - 2\,\hat{z}_{\hat{x}}\,\hat{z}_{\hat{\psi}}\,\hat{z}_{\hat{x}\hat{\psi}} + \hat{z}_{\hat{\psi}}^2\,\hat{z}_{\hat{x}\hat{x}} = -\hat{z}_{\hat{\psi}}^3\,f(\hat{\psi}). \tag{2.2}$$

In these variables, the velocity components are given by

$$\hat{u} = -\frac{1}{\hat{z}_{\hat{\psi}}} \quad \text{and} \quad \hat{w} = \frac{\hat{z}_{\hat{x}}}{\hat{z}_{\hat{\psi}}}.$$

Although the governing equation becomes more involved, the arbitrary distribution of vorticity — which is the source of nonlinearity of equation (2.1) — appears now as a variable coefficient, i.e. a function of the independent variable $\hat{\psi}$. Also, the domain is mapped into a rectangle as shown in figure (2.1). Although she points out the possibility of solving the problem by means of a Fourier expansion and perturbation techniques, the main purpose of her work was to prove the existence of a solution for arbitrary water depth, somehow extending Gerstner's theory. Dalrymple (1977) presented a solution to these equations using an iterative finite difference technique combined with a minimization procedure for the error at the dynamic free surface boundary condition.

From a practical point of view, Taylor (1955) addressed the problem of pneumatic breakwaters, a curtain of air bubbles which spread horizontally near the surface; it was observed that the height of waves was reduced when they propagated across the region of bubbles. He reasoned that these bubbles generated a current that would interact with the waves causing dissipation of wave energy. His theoretical study included two cases of current profile, constant and linear, distributed in a layer of depth $h$ near the free surface and vanishing elsewhere in the water column. It turns out, though, at first approximation, that the interaction between waves and a current is strongly influenced both by the speed of the current as well as by its vorticity near the free surface. This interaction is manifested particularly by a change in the dispersion relation.

Hunt (1955), considering perturbations on a turbulent flow like waves propagating on a river or a tidal current, studied the problem assuming a power law distribution for the current. If the flow is divided in two components, say the oscillatory wave motion given by the stream function

$$\hat{\psi} = \hat{\phi}(\hat{z})e^{ik(\hat{x}-c\hat{t})}$$

and a steady (prescribed) current, $U$, the linearized vorticity equation takes the form of Rayleigh (or inviscid Orr-Sommerfeld) equation

$$\hat{\phi}_{\hat{z}\hat{z}} - \left(k^2 + \frac{U_{\hat{z}\hat{z}}}{U - c}\right)\hat{\phi} = 0$$

which does not have a general solution for arbitrary current distribution $U$. In the above equation, $\hat{z}$ is the distance above the bottom, $k$ is the wave number, and $c$ the wave celerity. As Hunt observes, this linearized solution can be uniformly valid only for small amplitude waves and consequently he addresses the nonlinear case for shallow water waves.

Expanding both the current distribution and the stream function for the waves in power series of the vertical coordinate,

$$U(\hat{z}) = \sum_{1}^{\infty} \mathcal{U}_n \hat{z}^n \quad \text{and} \quad \hat{\psi}(\hat{x}, \hat{z}) = \sum_{1}^{\infty} \hat{\psi}_n(\hat{x}) \hat{z}^n,$$

and introducing into the vorticity equation

$$(U - c - \hat{\psi}_{\hat{z}})\nabla^2 \hat{\psi}_{\hat{x}} - \hat{\psi}_{\hat{x}}(U_{\hat{z}\hat{z}} - \nabla^2 \hat{\psi}_{\hat{z}}) = 0,$$

a sequence of relations between the functions $\hat{\psi}_n$ and the coefficients $\mathcal{U}_n$ is obtained, as well as the wave celerity. He finds the free surface profile, $\hat{\eta}$, governed by a variable coefficient Korteweg-de Vries equation

$$\begin{aligned} \eta \eta_x \left[ U_1'(U_1 - c_0) - \frac{3}{h}(U_1 - c_0^2) \right] - \frac{1}{3} \eta_{xxx} h^2 (U_1 - c_0^2) + \\ \eta_x \left[ -gh - hU_1'(U_1 - c) + (U_1 - c^2) \right] = 0, \end{aligned}$$

where $c$ is the wave celerity, $U_1$ is the surface velocity, $U_1'$ is the gradient of the current velocity at the surface, and

$$c_0 = U_1 - \frac{1}{2} h U_1' \pm \sqrt{gh + \frac{1}{4} h^2 U_1'^2},$$

where the +/− sign is to be chosen whether the waves propagate with or against the current. He then considers both cases of solitary and cnoidal waves, giving expressions for the celerity and the surface profile. The only shortcoming in Hunt's theory is the assumption that the current profile can be expanded in a power series with integer exponents about $\hat{z} = 0$; even so, he applies his results for a current with 1/7 power law distribution. The basis for his justification is the fact that the current has no singularity near the free surface; however, in his sequence of expansions some problem may be expected if the current is not analytic at the bottom.

For shallow water waves it would be desirable that no assumption be made about the current profile, except that no stagnation points should exist inside the fluid domain. Using the same equation as derived by Dubreil-Jacotin, Benjamin (1962) presented a solitary wave theory valid for currents with an arbitrary distribution of vorticity. At infinity, there is a mean steady current for which the stream function, $\hat{\Psi}$, is known, and the streamlines will be horizontal. Let this primary flow be denoted as

$$\hat{u} = W(\hat{s}) = -\hat{\Psi}'(\hat{s}),$$

where the $'$ represents differentiation. Recalling that the flow is steady in a frame of reference that follows the waves, a further change of variables is introduced, from the streamline $\hat{\psi}$ to the elevation $\hat{s}$ of the mean streamline $\hat{\Psi}$ at infinity; this is also the asymptotic value of the elevations $\hat{z}(\hat{x}, \hat{\psi})$. The governing equation thus becomes

$$W(\hat{s}) \left[ \left(1 + \hat{z}_{\hat{x}}^2\right) \hat{z}_{\hat{s}\hat{s}} - 2\, \hat{z}_{\hat{x}}\, \hat{z}_{\hat{s}}\, \hat{z}_{\hat{x}\hat{s}} + \hat{z}_{\hat{s}}^2\, \hat{z}_{\hat{x}\hat{x}} \right] + W'(\hat{s}) \left[ \hat{z}_{\hat{s}}^3 - \hat{z}_{\hat{s}} \left(1 + \hat{z}_{\hat{x}}^2\right) \right] = 0. \tag{2.3}$$

If variations in $\hat{x}$ are neglected, a uniform current is obtained for which the elevation of $\hat{z}$ is related to the velocity $W$ through

$$\hat{z}(\hat{s}) = \int_0^{\hat{s}} \frac{W(s)\, ds}{\sqrt{[W^2(s) - 2A]}},$$

where $A$ is a constant. The method then proceeds allowing $A$ to be a function of $\hat{x}$, as well as introducing a perturbation $B(\hat{x}, \hat{s})$,

$$\hat{z}(\hat{s}) = \int_0^{\hat{s}} \frac{W(s)\, ds}{\sqrt{[W^2(s) - 2A(\hat{x})]}} + B(\hat{x}, \hat{s}).$$

He concludes that, although vorticity may increase the wave celerity compared to the irrotational case, the effect is in general small for subcritical flows; however, the effects of vorticity for large Froude numbers may be significant on the wave properties, and he exemplifies with the case of standing waves.

In contrast to the wave theories discussed so far, in which an analytical solution is sought for an approximation of the problem, a different approach was developed by Dean (1965). In his Stream Function Wave Theory, valid for irrotational waves, the solution is assumed to have a Fourier expansion which satisfies exactly both the governing equation inside the fluid domain and the kinematic free surface boundary condition, but the coefficients of the series are determined numerically such that the root mean square error of the dynamic free surface boundary condition is minimized. This idea has since been applied by other authors (Chaplin (1980), Rienecker and Fenton (1981)) and even to unsteady wave trains, using the velocity potential (Lambrakos (1981)). Regarding rotational waves, Dalrymple (1973) applied the same methodology to the case of a current with a "bilinear shear" profile: a continuous, linear velocity distribution in two layers with different values of vorticity. In this case, a further matching condition has to be introduced at the interface. The governing equation is

$$\nabla^2 \hat{\psi} = \omega_0,$$

and the solution is assumed to have the form

$$\hat{\psi}(\hat{x},\hat{z}) = -(U_0 - c)(\hat{z} + h) - \frac{1}{2}\omega_0(\hat{z} + h)^2 + \sum_{n=1}^{N} X_n \sinh\left[nk(h+\hat{z})\right]\cos nk\hat{x}. \tag{2.4}$$

Besides the $X_n$ coefficients, the other unknowns of the problem are the wave length $L$ and the total discharge (or the value of the stream function at the free surface) $\hat{\psi}_\eta$. The free surface elevation, $\hat{\eta}$, is determined by solving the equation

$$\hat{\psi}_\eta = \hat{\psi}(\hat{x},\hat{\eta}(\hat{x})).$$

Later, Dalrymple and Cox (1976) solved the problem

$$\nabla^2 \hat{\psi} = \pm\gamma^2 \hat{\psi}$$

using the same technique, where the solution now was assumed to have the form

$$\hat{\psi}(\hat{x},\hat{z}) = \hat{\Psi}_{\pm}(\hat{z}) + \sum_{n=1}^{N} X_n \sinh\left[\left((nk)^2 \pm \gamma^2\right)^{\frac{1}{2}}(h+\hat{z})\right]\cos nk\hat{x}, \tag{2.5}$$

where the ± sign depends on on the sign in the governing equation and

$$\hat{\Psi}_{+}(\hat{z}) = \frac{1}{\gamma}(c - U_0)\sin\gamma(h+\hat{z})$$
$$\hat{\Psi}_{-}(\hat{z}) = \frac{1}{\gamma}(c - U_0)\sinh\gamma(h+\hat{z}).$$

They present results for values of dimensionless parameter $\gamma h$ ranging from .010 to .050 for deep water waves, and from .001 to .100 for shallow water cases, considering both following and opposing currents.

The experimental verification of these theories is extremely difficult, either because of lack of techniques for generation of a steady current with a specified vorticity profile, or because of measuring simultaneously flow velocities in two directions and gradients in velocities (in order to obtain the vorticity distribution).

From the mathematical point of view, this problem also poses very challenging questions with regard to the stability of the flow, existence of a solution for arbitrary current or interrelation between current profile and wave characteristics. The present work thus constitutes an effort to develop and investigate a particular solution of a very broad and complex problem.

# CHAPTER 3
# FORMULATION OF THE THEORY

## 3.1 Mathematical Formulation

Consider long crested waves of permanent form propagating on an inviscid and incompressible fluid of constant depth, such that in a frame of reference which follows the waves, the motion is steady and two dimensional. Also, a steady mean current is allowed to exist. In this case, the streamlines coincide with the trajectories of fluid particles and vorticity will be conserved.

For the remainder of this chapter, the coordinate axes are placed at the mean water level, the water depth will be represented as $h$, the wave height as $H$, the surface elevation as $\hat{\eta}$, and the wave length as $L$. The positive horizontal direction indicates the propagation of the wave with respect to the bottom. Figure (3.1) shows schematically the problem being considered. The stream function, $\hat{\psi}$, allows

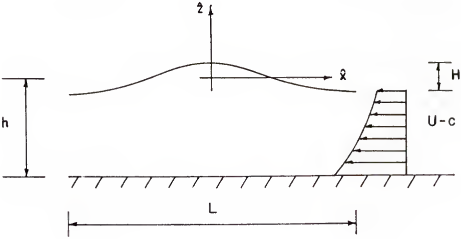

Figure 3.1: Flow schematization.

any arbitrary flow to be described by a single equation

$$\hat{\psi}_{\hat{z}}\,\nabla^2\hat{\psi}_{\hat{x}} \;-\; \hat{\psi}_{\hat{x}}\,\nabla^2\hat{\psi}_{\hat{z}} \;=\; 0, \tag{3.1}$$

equivalent to the more usual form

$$\nabla^2\hat{\psi} \;=\; f(\hat{\psi}),$$

which states the vorticity is conserved along each streamline. For irrotational motions, the arbitrary function $f$ is taken as identically zero.

Next, dimensionless variables will be introduced according to the following scaling:

$$\begin{array}{lll} x = \dfrac{\lambda\hat{x}}{L}\,; & z = \dfrac{\hat{z}}{h}\,; & \eta = \dfrac{\hat{\eta}}{H}\,; \\[2ex] \psi = \dfrac{\hat{\psi}}{H\sqrt{gh}}\,; & \omega = \dfrac{\hat{\omega}}{H/h\sqrt{g/h}}\,; & P = \dfrac{\hat{p} + \rho g\hat{z}}{\rho g H/2}\,; \end{array}$$

where the following nondimensional parameters will be used hereafter:

$\lambda$ : period of the function $\mathrm{lcc}(x, \gamma_2)$;

$k = \lambda/L$ : wave number;

$\epsilon = kh$ : relative water depth;

$\alpha = H/h$ : ratio of wave height to water depth;

where the meaning of lcc- will be defined later. In these variables, the problem can be formulated as:

$$\psi_z\psi_{zzx} - \psi_x\psi_{zzz} + \epsilon^2\psi_z\psi_{xxx} - \epsilon^2\psi_x\psi_{xxz} = 0. \tag{3.2}$$

for $-\infty < x < \infty$ and $-1 \le z \le \alpha\eta(x)$ ; the boundary conditions are:

$$\psi \;=\; 0 \qquad \text{, at } z = -1 \tag{3.3}$$

$$\psi \;=\; \psi_\eta \qquad \text{, at } z = \alpha\eta(x) \tag{3.4}$$

$$\eta + \frac{1}{2}\alpha\left(\psi_z^2 + \epsilon^2\psi_x^2\right) \;=\; Q \qquad \text{, at } z = \alpha\eta(x) \tag{3.5}$$

Among the solutions of the problem above, a particular case will be considered, namely those $\psi(x,z)$ which can be formally expressed as a product of a function $X(x)$ and a function $Z(z)$:

$$\psi\,(x,z) \;=\; A\,X(x)\,Z(z).$$

The method of separation of variables applied to equation (3.2) yields:

$$\frac{Z\,Z''' \;-\; Z'\,Z''}{Z\,Z'} \;=\; \epsilon^2\frac{X\,X''' \;-\; X'\,X''}{X\,X'} \;=\; \text{constant}. \tag{3.6}$$

The separation constant must be real, and can be taken as positive, negative or equal to zero. In Appendix A, the different solutions are discussed corresponding to each case. For the solution in the moving frame of reference to represent a progressive wave relative to a fixed observer, the following conditions have to be satisfied. First, the horizontal velocity must not vanish inside the fluid domain: as a consequence, the function $X$ has to be different from zero for any value of $x$. Second, the vertical velocity must be identically zero along the bottom: therefore, the function $Z$ has to vanish for some value of $z$. Third, the solution must be bounded inside the fluid domain.

Based on these conditions, according to the development in Appendix A, the separation constant is negative. The solutions $X$ and $Z$ will depend on parameters, respectively $\gamma_2$ and $\delta_2$, which in that Appendix are generically referred to as $\tilde{c}_2$. Further, if the stream function is expressed as

$$\psi \;=\; \frac{1}{\delta_1}\,X(x;\gamma_2)\,Z(z+1;\delta_2) \tag{3.7}$$

$\gamma_2$ varies strictly between -0.1839 ($= \;-1/(2\mathrm{e})$) and 0, while $\delta_2$ has to be greater than 0. For the limiting value of $\gamma_2$ equal to -0.1839, the function $X$ reduces to a constant, in other words, there is no variation along the horizontal coordinate. Similarly, for $\delta_2$ equal to zero, the solution reduces to a steady current for reasons which will be shown later.

The choice of scaling parameters allows the separation constant to be equal to $-\epsilon^2$. The function $X$, which can be expressed as

$$X(x;\gamma_2) = X_1\, lcc(x;\gamma_2),$$

satisfies the differential equation

$$X'' + X\log|X| + \frac{1}{2}X = 0 \tag{3.8}$$

or, equivalently,

$$(X')^2 + X^2\log|X| = \gamma_2. \tag{3.9}$$

The maximum and minimum values of $X$ are, respectively, $X_1$ and $X_0$, which are related to $\gamma_2$ by the expressions

$$X_1^2\log X_1 = X_0^2\log X_0 = \gamma_2. \tag{3.10}$$

Figure (3.2) shows the graph of $X$ normalized by its maximum value, $X_1$: it is a periodic even function, its period $\lambda$ depends on $\gamma_2$, and, for future reference, it will be denoted as $lcc$– referred to as "logarithmic cosine" due to its similarity with the circular cosine. Table (B.1) in Appendix A presents values of $X_0$, $X_1$, $\overline{X(x;\gamma_2)}$, and $\lambda$ for different values of $\gamma_2$.

Similar relations hold for the function $Z$ which gives the vertical structure of the stream function. It satisfies the same differential equation,

$$Z'' + Z\log|Z| + \frac{1}{2}Z = 0 \tag{3.11}$$

or, equivalently,

$$(Z')^2 + Z^2\log|Z| = \delta_2, \tag{3.12}$$

the only difference being that $\delta_2$ has to be greater than zero. Choosing the value of $Z$ to be zero at the bottom is equivalent to a translation of origin. Figure (3.3) shows the graph of $Z$ normalized by its maximum value, $Z_1$, and, for future reference it will be referred as *lsc*−, referred to as "logarithmic sine" since it is an odd, periodic function with period $\mu$, similar to the circular sine. Also, the following relation between $Z_1$ and $\delta_2$ holds:

$$Z_1^2 \log Z_1 \;=\; \delta_2. \tag{3.13}$$

Figure (3.4) is the phase plane for the functions $X$ and $Z$ and qualitatively summarizes their behavior. In figures (3.2), (3.3), and (3.4), the general variable $Y(y;\tilde{c}_2)$ is used to denote either $X(x;\gamma_2)$ or $Z(z;\delta_2)$.

Using the differential relations presented above, the boundary conditions at the free surface are finally expressed as

$$\psi_\eta \;=\; \frac{1}{\delta_1} X\, Z \tag{3.14}$$

$$\eta \;+\; \frac{\alpha\epsilon^2}{2\delta_1^2}\left(\delta_2 X^2 \;+\; \gamma_2 Z^2\right) \;=\; Q \quad , \text{at } z \;=\; \epsilon(1 \;+\; \alpha\eta(x)). \tag{3.15}$$

The problem then reduces to finding constants $\gamma_2$, $\delta_1$, and $\delta_2$ as well as a function $\eta(x)$ such that both the kinematic and dynamic boundary conditions are satisfied.

Now it becomes easier to identify the limiting case for $\delta_2$ equal to zero. As shown in Appendix A, the function $Z$ becomes

$$Z(z;0) \;=\; \exp\left(-\frac{1}{4}z^2\right),$$

which apparently would be a suitable choice for deep water waves. However, in equation (3.15), the explicit dependency on the horizontal coordinate disappears; multiplying both sides of this equation by $\alpha$ and adding 1, (3.15) assumes the form

$$\varsigma \;+\; \frac{1}{2}\left(\frac{\alpha\epsilon}{\delta_1}\right)^2 \gamma_2 Z(\varsigma;0) \;=\; Q',$$

where $\varsigma \;=\; 1 \;+\; \alpha\eta$ and $Q' \;=\; 1 \;+\; \alpha Q$, which has only the trivial solution $\eta \;=$ constant. This poses an important question, whether a solution would exist in an arbitrary finite depth. The answer does not seem to be immediate, hence the approach adopted was to search for the numerical evidence of existence of a non trivial solution, in other words, a periodic rotational motion.

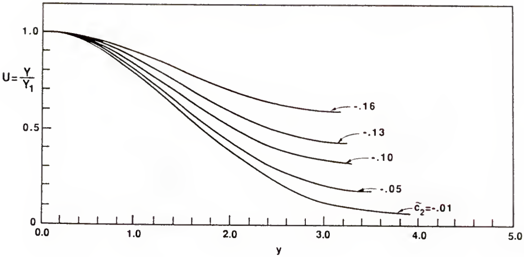

Figure 3.2: Function $lcc(y; \tilde{c}_2)$

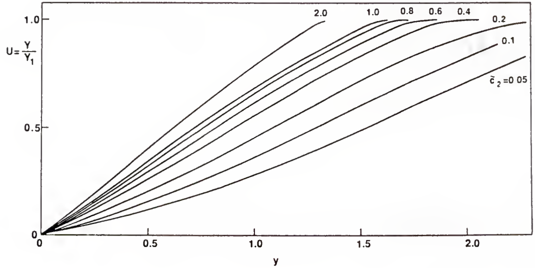

Figure 3.3: Function $lsc(y; \tilde{c}_2)$

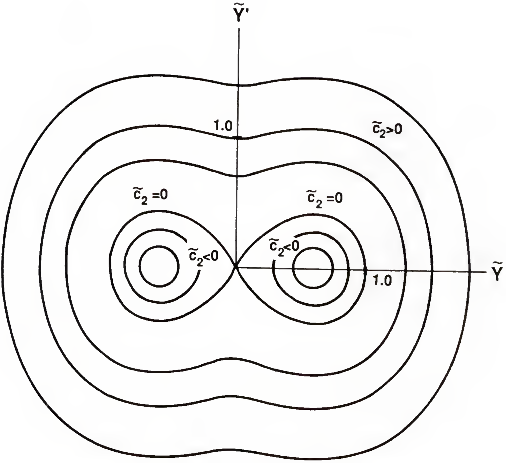

Figure 3.4: Phase plane trajectories

## 3.2 Numerical Formulation

The basic idea of the theory developed by Dean (1965) for irrotational waves is to express the solution of the full non linear problem in a series of functions which would satisfy the governing equation inside the fluid domain but not the dynamic condition at the free surface. The unknown coefficients of the series would then be determined through a minimization procedure of the mean quadratic error on the dynamic free surface boundary condition (DFSBC). In its original formulation, Dean used the Bernoulli constant as the convergence parameter, letting the wave height adjust freely. Later, Dalrymple (1973) made a significant improvement on this theory extending it in order to include a current with constant vorticity. He also introduced two constraints on the minimization of the objective function: one on the mean water level and another on the wave height. Using the method of Lagrangian multipliers, the wave height became one of the specified parameters.

Basically, the same methodology will be adopted here. Once the wave height, the water depth and the total discharge are specified, the parameters $\gamma_2$, $\delta_1$, $\delta_2$, and $\epsilon$ are determined such that the objective function, $\mathcal{O}$,

$$\mathcal{O} \;=\; \frac{2}{\lambda}\int_0^{\lambda/2} \left(Q-\overline{Q}\right)^2 \, \mathrm{d}x \;+\; l_1\left(|\eta(0)\;-\;\eta(\lambda/2)|\;-\;1\right) \;+\; l_2\frac{2}{\lambda}\int_0^{\lambda/2} \eta \, \mathrm{d}x \qquad (3.16)$$

is minimized. The constants $l_1$ and $l_2$ are Lagrange multipliers and the overbar means average over the wave length. The first constraint specifies that the difference between maximum and minimum surface elevations should be equal to 1 — since the free surface displacement has been scaled by the wave height. The second constraint specifies that the mean free surface elevation be equal to zero.

The solution is achieved by an iterative procedure. At each iteration, the free surface is updated through the kinematic free surface boundary condition (KFSBC), equation (3.14), and the new value of the objective function, equation (3.16), is computed.

New values of the parameters are then computed using a method based on a nonlinear least squares method. Because the derivatives of the functions *lcc*− and *lsc*− with respect to the parameters $\gamma_2$ and $\delta_2$, respectively, are not evaluated, the method being used cannot be properly named nonlinear least squares but it follows the same basic idea. Let $\xi_i^n$ generically denote one of the four varying parameters at iteration $n$; then

$$\mathcal{O}^{n+1} = \mathcal{O}^n + \sum_{i=1}^{4} \left(\frac{\partial \mathcal{O}}{\partial \xi_i}\right)^n \Delta\xi_i^n + \left(\frac{\partial \mathcal{O}}{\partial l_1}\right)^n \Delta l_1^n + \left(\frac{\partial \mathcal{O}}{\partial l_2}\right)^n \Delta l_2^n. \tag{3.17}$$

At the minimum, the variation of the objective function with respect to the parameters and the Lagrange multipliers should be zero. Therefore, taking the derivatives

$$\begin{aligned} 0 = {} & \frac{\partial \mathcal{O}^{n+1}}{\partial \xi_j^n} \\ = {} & \frac{\partial \mathcal{O}^n}{\partial \xi_j^n} + \sum_{i=1}^{4} \frac{\partial^2 \mathcal{O}^n}{\partial \xi_j^n \partial \xi_i^n} \Delta\xi_i^n \\ & + \frac{\partial^2 \mathcal{O}^n}{\partial \xi_j^n \partial l_1^n} \Delta l_1^n + \frac{\partial^2 \mathcal{O}^n}{\partial \xi_j^n \partial l_2^n} \Delta l_2^n \quad , \end{aligned} \tag{3.18}$$

gives a system of six equations in six unknowns, the increments in the four parameters and the two Lagrange multipliers. The expressions for the partial derivatives in the previous equation are given in Appendix C.

The procedure stops when the relative change in the mean quadratic error in the DFSBC is less than $10^{-3}$. In several cases, however, the procedure turned out to be unstable, in the sense that the error would tend to increase. A possible explanation is the fact mentioned before regarding the derivative of the functions with respect to their parameters. In these cases, a trial and error procedure was attempted, imposing small variations in only one of the parameters at each time, and choosing the direction in which the objective function $\mathcal{O}$ would be smallest.

The starting values adopted for the iterations are derived from an analogy between these waves and the (irrotational) linear wave theory. These relations are presented and discussed in the next section.

## 3.3 Analytical Properties

Before deriving the expressions for physical quantities, it might be worthwhile examining some of the analytical properties of the solution and establishing analogies between the present theory and the theory for irrotational waves. By doing so, it may be possible to increase the physical understanding about the present theory, and ultimately derive relations between the theoretical parameters and physical quantities like wave height, water depth, wave period, and total discharge. Also, such relations might bring about an improvement of the numerical model, since better estimates for the initial values of the theoretical parameters would be available.

Evaluating the DFSBC at crest and trough yields

$$\begin{aligned} \text{crest:} \quad & \eta_c + \frac{1}{2}\frac{\alpha\epsilon^2}{\delta_1^2}\left(\delta_2 X_0^2 + \gamma_2 Z_c^2\right) = Q \\ \text{trough:} \quad & \eta_t + \frac{1}{2}\frac{\alpha\epsilon^2}{\delta_1^2}\left(\delta_2 X_1^2 + \gamma_2 Z_t^2\right) = Q. \end{aligned}$$

Subtracting both expressions, using equation (3.14), and observing that, in dimensionless variables $\eta_c - \eta_t = 1$, the following relation between the parameters should hold:

$$\alpha\epsilon^2 \, \frac{X_1^2 - X_0^2}{2}\left(\frac{\delta_2}{\delta_1^2} - \frac{\gamma_2}{X_0^2 X_1^2}\psi_\eta^2\right) = 1. \qquad (3.19)$$

The above expression is used for verification of the results and to give the initial value for $\psi_\eta$ in the numerical procedure.

A major characteristic of the present stream function is the fact that it is composed only of the product of two functions, in contrast for instance to Dean's theory which uses a sum of terms. For irrotational waves, the stream function is expressed in dimensional variables as

$$\hat{\psi}(\hat{x},\hat{z}) = -(U-c)\,(\hat{z}+h) + \sum_{n=1}^{N} A_n \sinh\left[nk(h+\hat{z})\right]\cos nk\hat{x} \qquad (3.20)$$

In this case, there is a mean part — which represents the current and the effect of translating the reference frame — and an oscillatory part. The same, however, is not so evident for the present theory, unless one recalls that the function $X$ has a strictly positive mean value.

Considering Airy's theory, which corresponds to the first two terms in equation (3.20), the velocities at the crest, $\hat{u}_c$, and at the trough, $\hat{u}_t$, are, respectively,

$$\begin{aligned}\hat{u}_c &= U - c + \frac{Hgk}{2\sigma}\frac{\cosh[k(h+z)]}{\cosh kh} \\ \hat{u}_t &= U - c - \frac{Hgk}{2\sigma}\frac{\cosh[k(h+z)]}{\cosh kh}\end{aligned}$$

Further, considering shallow water approximation, the ratio between the amplitude of oscillation and the mean velocity is

$$\frac{\hat{u}_c - \hat{u}_t}{\bar{\hat{u}}} = \frac{Hgk}{\sigma}\frac{1}{U-c} = -\frac{H}{h}. \tag{3.21}$$

For the present theory, the velocities at the crest and at the trough are,

$$\begin{aligned}\hat{u}_c &= AX_0Z'(\epsilon(1+z);\delta_2) \\ \hat{u}_t &= AX_1Z'(\epsilon(1+z);\delta_2)\end{aligned}$$

where $A$ is a constant. Then, the ratio between the amplitude of oscillation and the mean value is

$$\frac{\hat{u}_c - \hat{u}_t}{\bar{\hat{u}}} = \frac{X_0 - X_1}{\bar{X}} \tag{3.22}$$

Because the right-hand side of (3.22) is a function of $\gamma_2$ only, it is acceptable to compare this equation with (3.21) as a first approximation:

$$\frac{X_1 - X_0}{\bar{X}} = \frac{H}{h}, \tag{3.23}$$

which gives a relationship between $\gamma_2$ and $\alpha$, the ratio between wave height and water depth.

As will be presented in Chapter 4, the application of (3.23) resulted in very good estimates for $\gamma_2$ and in low values for the mean quadratic error on the DFSBC. Therefore, it might be justified to try a perturbation expansion of the boundary conditions, in a procedure similar to Stokes' waves.

The combined free surface boundary condition (CFSBC) expressed in dimensionless variables, valid for any steady two-dimensional flow of an incompressible fluid, is given by

$$\psi_x - (\alpha\epsilon)^2\psi_x\psi_z\psi_{xx} + (\alpha\epsilon)^2\psi_x^2\psi_{xz} - \alpha^2\psi_z^2\psi_{xz} + \alpha^2\psi_x\psi_z\psi_{zz} = 0, \text{ at } z = \alpha\eta. \quad (3.24)$$

Expressing the stream function as in (3.7) as well as using the differential relations for $X$ and $Z$, the CFSBC for the present flow becomes

$$Z + \frac{(\alpha\epsilon)^2\epsilon}{\delta_1^2}Z'\left[\gamma_2 Z^2 - \delta_2 X^2\right] = 0, \text{ at } z = \epsilon(1 + \alpha\eta) \quad (3.25)$$

Next, $X$ and $\eta$ will be expanded in a Fourier series, and $Z(\epsilon(1 + \alpha\eta);\delta_2)$ will be expanded in a Taylor series about $z = \epsilon$. Let

$$\begin{array}{rclclclc} \eta(x) & = & \eta_0(x) & + & \alpha\epsilon\,\eta_1(x) & + & (\alpha\epsilon)^2\,\eta_2(x) & + \cdots \\ X(x;\gamma_2) & = & \overline{X}(\gamma_2) & + & a_1\cos(\frac{2\pi x}{\lambda}) & + & a_2\cos(\frac{4\pi x}{\lambda}) & + \cdots \\ Z(\epsilon + \alpha\epsilon\eta;\delta_2) & = & Z(\epsilon;\delta_2) & + & \alpha\epsilon\eta\,Z'(\epsilon;\delta_2) & + & \frac{1}{2}(\alpha\epsilon)^2\eta^2\,Z''(\epsilon;\delta_2) & + \cdots \end{array} \quad (3.26)$$

It has been implicitly assumed that $\overline{X} = O\ (\alpha)^{-1}$, $a_1 = O\ (1)$, $a_2 = O\ (\alpha)$, and so on. Substituting these expressions into the CFSBC, equation (3.25), terms of same order of magnitude in $(\alpha)$ will be grouped together. To lowest order, the relation obtained is analogous to the dispersion relation in Stokes'waves:

$$\frac{Z(\epsilon;\delta_2)}{Z'(\epsilon;\delta_2)} = (\alpha\epsilon)^2\epsilon\frac{\delta_2}{\delta_1^2}\overline{X}^2(\gamma_2). \quad (3.27)$$

To next order, the first order free surface displacement is obtained:

$$\left\{\frac{Z\,Z''}{Z'} - Z'\right\}\eta_0(x) + 2a_1\alpha\epsilon^2\frac{\delta_2}{\delta_1^2}\overline{X}(\gamma_2)Z'\cos(\frac{2\pi x}{\lambda}) = 0, \quad (3.28)$$

where the function $Z$ and its derivatives are computed at $\epsilon$. From the relations between $Z$ and its derivatives presented in section 3.1, the term between brackets is negative. The coefficient multiplying $\cos(2\pi x/\lambda)$ is positive. Consequently, the first order elevation, $\eta_0$, behaves as a cosine function, having its maximum at $x = 0$.

For reasons which will be clear in the next section, it turns out that $\eta$, the total free surface elevation, must have its maximum at $x = \lambda/2$, in other words, $\eta_0$ must be proportional to $-\cos(2\pi x/\lambda)$. Therefore, equation (3.28) can not be satisfied, and the perturbation expansion breaks down.

## 3.4 Derived Physical Quantities

### 3.4.1 Vorticity Distribution

In dimensionless variables, the vorticity is given as

$$\omega = -(\psi_{zz} + \epsilon^2 \psi_{xx}).$$

Expressing the stream function as in (2.1) and using the differential equations which govern the functions $X$ and $Z$, the vorticity is finally written as

$$\begin{aligned} \omega &= -\epsilon^2(\psi + \psi \log \delta_1 \psi) \\ &= -\frac{\epsilon^2}{\delta_1} X(x;\gamma_2) Z(\epsilon(1+z);\delta_2) \{ 1 + \log [X(x;\gamma_2) Z(\epsilon(1+z);\delta_2)] \}. \end{aligned} \quad (3.29)$$

Although the vorticity distribution is given in terms of the stream function, as shown in figure (3.5), it is always possible to identify an average elevation for each streamline and therefore obtain, to some extent, a qualitative distribution of vorticity with depth. At the bottom, its value is zero but it has an infinite gradient. Depending on the total discharge, i.e. the value of the stream function at the free surface, there may exist an elevation — or a streamline — which divides the flow in two regimes, each with opposite signs of vorticity.

It should be emphasized here that both the vertical gradient of the horizontal velocity, $u_z$, and the horizontal gradient of the vertical velocity, $w_x$, contribute to the total vorticity. Each of these terms is not constant along the streamlines, although their difference, $u_z - w_x$, is. For the present theory, it is possible to express analytically each of these terms along a given streamline $\psi_0$:

$$u_z = -\frac{\epsilon^2}{\delta_1} X Z'' = \epsilon^2 \psi_0 \left[ \frac{1}{2} + \log \delta_1 \psi_0 - \log X(x;\gamma_2) \right] \quad (3.30)$$

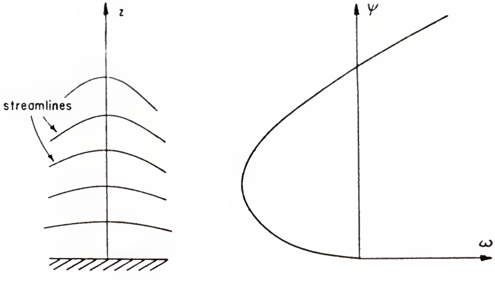

Figure 3.5: Vorticity distribution.

$$\epsilon^2 w_x = \frac{\epsilon^2}{\delta_1} X'' Z = -\epsilon^2 \psi_0 \left[ \frac{1}{2} + \log X(x;\gamma_2) \right] . \qquad (3.31)$$

If at a fixed elevation (or a fixed streamline), the averages of equations (3.30) and (3.31) are computed along the wave length, the results differ from the total average vorticity.

This property is not unique to this theory. In the Stream Function Wave Theory for waves on a constant shear current (equation (2.4)), all the contribution to vorticity is given by the "current" part of the stream function. However, in Dalrymple and Cox's theory (equation (2.5)), there is also a contribution from the gradients in vertical velocity which does not vanish when averaged over the wave length.

In other words, if only a profile of horizontal velocities is measured and averaged over a wave period, the "apparent vorticity" computed by taking the gradient of these velocities would be different from the actual vorticity in the flow. As it will be shown in the derivation of pressure, vorticity is a quantity which has an effect on the dynamics of the flow. As a consequence, neglecting a detailed measurement of the velocity field constitutes a major difficulty in obtaining any experimental verification for a theory whose formulation is based on vorticity.

### 3.4.2 Horizontal Velocity

The total horizontal velocity $u$, determined as

$$u = -\epsilon\psi_z = -\frac{\epsilon}{\delta_1} X Z'$$

includes three components: the first is equal to the celerity of the wave with negative sign, due to the motion of the reference frame; the second is a mean current which, below trough level, can be defined as the average over the wave length; finally, an oscillatory part, which is identified with the wave motion. In general, this total velocity should always be opposite to the direction of wave propagation (negative in the present convention.)

At a given elevation below the trough, for instance at the bottom, the maximum total velocity should occur under the trough, whereas the minimum should occur under the crest. Recalling from Appendix B that $X(x;\gamma_2)$ is a decreasing function between 0 and $\lambda/2$ which varies from $X_1$ to $X_0$, respectively, it can be shown that the trough should occur at $x = 0$ with the crest at $x = \lambda/2$. Indeed,

$$\begin{aligned} \max|u_b| &= |u_{b,t}| \propto X_1 Z'(0;\delta_2) \\ \min|u_b| &= |u_{b,c}| \propto X_0 Z'(0;\delta_2) \end{aligned}$$

thus proving the previous statement. Figure (3.6) shows an example for a weak following current; a similar conclusion is valid for an opposing current. An interesting case would happen if the current were so strong that the wave celerity relative to a fixed observer were less than the (vertical) average velocity. This situation is similar to Case D, discussed by Peregrine (1976). The total mass transport would be in the positive direction and, in the definition of the stream function, $X$ should be taken with a negative value. In this case, the maximum velocity in magnitude would occur at the crest.

### 3.4.3 Mean Horizontal Velocity

At a fixed elevation below trough level, the mean horizontal velocity is proportional to the mean value of the function $X(x;\gamma_2)$

$$(U-c)|_z \;=\; -\frac{\epsilon}{\delta_1}\overline{X}(\gamma_2)\, Z'(\epsilon(1+z);\delta_2). \tag{3.32}$$

So, the ratio between mean velocities at a given elevation and, for instance, at the bottom is fixed

$$\frac{(U-c)|_z}{(U-c)|_0} \;=\; \frac{Z'(\epsilon(1+z);\delta_2)}{Z'(0;\delta_2)} \;=\; K. \tag{3.33}$$

However, this is the same ratio between total velocities. Therefore,

$$\begin{aligned} (U-c+u')|_z \;&=\; K\,(U-c+u')|_0 \qquad\qquad \div(U-c)|_0 \\ \Rightarrow \qquad \frac{u'|_z}{u'|_0} \;&=\; K, \end{aligned}$$

the oscillatory component of velocity at all horizontal locations has a vertical distribution similar to the one of the total mean current, which is an unexpected result.

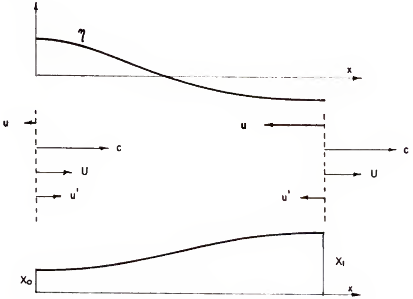

Figure 3.6: Relative position of free surface elevation and horizontal velocity at the bottom.

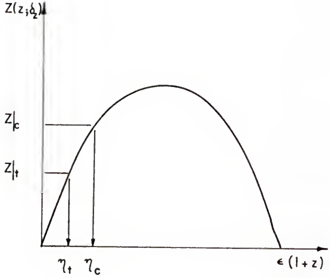

Figure 3.7: Determination of $\eta$

### 3.4.4 Free Surface Profile

The free surface $\eta$ is determined from the kinematic boundary condition. Again, recalling the behavior of $X(x;\gamma_2)$ between 0 and $\lambda/2$, because the free surface is a streamline,

$$\left.\begin{array}{rrcl} \text{at trough:} & X_1 Z|_t & = & \delta_1 \psi_\eta \\ \text{at crest:} & X_0 Z|_c & = & \delta_1 \psi_\eta \end{array}\right\} \Rightarrow \quad Z|_c > Z|_t .$$

Since the crest elevation by definition has to be higher than the trough elevation, figure (3.7) shows why the ascending part of the function $Z$ should be used in order to compute the free surface $\eta$.

### 3.4.5 Pressure

For steady, two dimensional flows with vorticity, the inviscid equations of motion can be integrated, yielding an expression similar to Bernoulli's equation. In dimensional variables, Euler's equations can be written as

$$\left\{ \begin{aligned} \frac{1}{2}(\hat{u}^2 + \hat{w}^2)_{\hat{x}} + (\hat{u}_{\hat{z}} - \hat{w}_{\hat{x}})\,\hat{w} &= -\frac{1}{\rho}\hat{p}_{\hat{x}} \\ \frac{1}{2}(\hat{u}^2 + \hat{w}^2)_{\hat{z}} - (\hat{u}_{\hat{z}} - \hat{w}_{\hat{x}})\,\hat{u} &= -\frac{1}{\rho}\hat{p}_{\hat{z}} - g \end{aligned} \right. \tag{3.34}$$

Taking into account that

$$\hat{u} = -\hat{\psi}_{\hat{z}} \qquad \text{and} \qquad \hat{w} = \hat{\psi}_{\hat{x}}$$

as well as the fact that the vorticity $(\hat{u}_{\hat{z}} - \hat{w}_{\hat{x}})$ is a function of the streamline only,

$$\hat{\omega} = -\nabla^2\hat{\psi} = f(\hat{\psi}),$$

the system of equations (3.34) reduces to

$$\nabla\left[\frac{1}{2}(\hat{u}^2 + \hat{w}^2) + \frac{\hat{p}}{\rho} + g\,\hat{z} + \int^{\hat{\psi}} f(s)\mathrm{d}s\right] = 0,$$

valid throughout the fluid domain. Although each term inside the bracket depends on the stream function, the entire bracket does not depend on the particular point (or streamline) being considered, and the form of Bernoulli's equation is finally obtained:

$$\frac{1}{2}(\hat{u}^2 + \hat{w}^2) + \frac{\hat{p}}{\rho} + g\,\hat{z} + \int^{\hat{\psi}} f(s)\mathrm{d}s = \hat{Q}. \tag{3.35}$$

Since the function $f$ is determined from equation (3.29), the integration can actually be carried out in analytical terms, and the pressure determined as

$$\frac{\hat{p}}{\rho} = g\,(\hat{\eta} - \hat{z}) + \frac{1}{2}\left[(\hat{u}^2 + \hat{w}^2)|_{\hat{\eta}} - (\hat{u}^2 + \hat{w}^2)|_{\hat{z}}\right] + \frac{k^2}{2}\hat{\psi}^2(\log\delta_1\hat{\psi} - \frac{1}{2})|_{\psi}^{\psi_\eta}. \tag{3.36}$$

The dimensionless dynamic pressure is expressed as

$$P(x,z) = 2\eta + \frac{\alpha\epsilon^2}{\delta_1^2}\left(\gamma_2 + \frac{1}{2}X^2\right)\left(Z|_\eta^2 - Z^2\right). \tag{3.37}$$

# CHAPTER 4
# NUMERICAL RESULTS

## 4.1 Introduction

Because the existence of a solution for the problem given by equations (3.14)-(3.15) could not be proven analytically, numerical experiments were carried out in order to find a possible solution. The mean quadratic error at the dynamic free surface boundary condition (DFSBC) is used to quantify how well the conditions of the problem are satisfied, or how good the approximation is.

The cases that have been considered are summarized in table (4.1) which gives the specified physical parameters — water depth, wave height, and wave period. The theoretical parameters used in the present theory — $\gamma_2$, $\delta_1$, and $\delta_2$ — as well as the dimensionless total discharge, $\psi_\eta$, and relative water depth, $\epsilon$, are listed in table (4.2). They were chosen such that the ratio of wave height to water depth ($\alpha$) had different values, except for Case 2A which differs from Case 2 only for the parameters $\delta_1$ and $\delta_2$; as shown later, such change causes the mean current to have a different profile. For each case, sections of the error surface are computed, as well as the constraints on the mean water level and wave height, mentioned in section 3.4.

The first tests aimed to quantify the influence of the several parameters on the DFSBC error as well as to verify how they were interrelated. Then, for sufficiently small values of this error, the velocity profile is computed. From this profile, the mean velocities at the bottom and at the trough level are obtained to define a constant shear current which will be used with the Stream-Function Wave Theory — from now on referenced as SFWT — developed by Dalrymple (1973). The two

Table 4.1: Wave parameters for cases studied.

| Case | wave height $H$ (m) | water depth $h$ (m) | wave period $T$ (s) |
|---|---|---|---|
| 1 | 1.453 | 2.00 | 6.0 |
| 2 | 5.237 | 10.0 | 10. |
| 2A | 5.237 | 10.0 | 10. |
| 3 | 1.290 | 4.42 | 8.0 |
| 4 | 1.800 | 12.2 | 12. |

Table 4.2: Theoretical parameters for cases studied.

| Case | $\gamma_2$ | $\delta_1$ | $\delta_2$ | $\psi_\eta$ | $\epsilon$ |
|---|---|---|---|---|---|
| 1 | -0.140 | 0.1129 | 1.279 | 1.220 | 0.2258 |
| 2 | -0.160 | 0.1514 | 1.213 | 1.796 | 0.4158 |
| 2A | -0.160 | 0.05048 | 0.1260 | 1.796 | 0.4158 |
| 3 | -0.175 | 0.1172 | 0.3764 | 2.996 | 0.8638 |
| 4 | -0.180 | 0.08492 | 0.0500 | 4.300 | 1.693 |

theories will then be compared for velocity field, pressure, wave length, and free surface elevation.

Because the SFWT is a n-th order theory, which has more degrees of freedom to adjust to the free surface boundary conditions, results are also presented for the first order SFWT — from now on referenced as SFWT (1) — with the same constant shear current. This first order theory has only one Fourier component, which implies, for instance, that the horizontal velocities at crest and at trough are equal in magnitude. However, it incorporates some degree of nonlinearity by satisfying exactly the kinematic free surface boundary condition, in contrast with Airy's theory which also has only one Fourier component.

As a mean to check the validity of the present theory and the fitness of the theoretical parameters, the dimensionless mean quadratic error at the DFSBC, the dimensionless wave height, and the mean free surface elevation were computed: for a true solution, these two last values should be equal, respectively, to 1.0 and zero. The left hand side of equation (3.19), derived from the DFSBC evaluated at crest

Table 4.3: Validity of the solution.

| Case | RMS error | | | H | $\overline{\eta}$ | Eq. |
|---|---|---|---|---|---|---|
| | SFWT (N) | SFWT (1) | Present theory | | (m) | (3.19) |
| 1 | $4.64 \times 10^{-4}$ (16) | $8.95 \times 10^{-2}$ | $8.97 \times 10^{-2}$ | 0.9956 | -0.060 | 0.9611 |
| 2 | $2.87 \times 10^{-4}$ (7) | $6.12 \times 10^{-2}$ | $5.96 \times 10^{-2}$ | 0.9904 | -0.011 | 0.9743 |
| 2A | $3.43 \times 10^{-4}$ (8) | $6.08 \times 10^{-2}$ | $5.24 \times 10^{-2}$ | 0.9309 | -0.002 | 0.9155 |
| 3 | $6.74 \times 10^{-5}$ (4) | $2.11 \times 10^{-2}$ | $2.38 \times 10^{-2}$ | 0.9939 | -0.017 | 0.9931 |
| 4 | $5.54 \times 10^{-5}$ (3) | $2.30 \times 10^{-3}$ | $4.31 \times 10^{-3}$ | 1.010 | 0.004 | 0.9989 |

and at trough, is also listed; theoretically, it should be equal to 1. Table (4.3) summarizes these results, and also give the root mean square error for both orders of SFWT. The error for the high order SFWT was smaller by two or three orders of magnitude, but the values for the present theory and the SFWT (1) were practically the same.

## 4.2 Influence of $\delta_1$ and $\delta_2$

Figure (4.1) shows a typical example of how the quadratic mean error in the DFSBC varies for different values of $\delta_1$ and $\delta_2$. All other parameters — the total discharge, the relative water depth, and $\gamma_2$ — were held constant. The ratio wave height to water depth had a different value for each case (except cases 2 and 2A), and $\gamma_2$ was chosen according to equation (3.23) resulting in the values for $\gamma_2$ listed in table (4.2).

From that figure, there seems to be a relation between $\delta_1$ and $\delta_2$, represented by the solid line, which reduces the error. However, such curve does not correspond to a locus of minima because the error itself tends to decrease with decreasing values of $\delta_1$, while the wave height is kept equal to 1 (in dimensionless variables) and the mean water level is approximately zero.

This is a paradoxical result for it indicates that the minimum might occur at $\delta_2$ equal to zero. But, in section 3.1, it was shown that, in such case, no periodic solution exists. Therefore, the error surface must have a singularity at the origin, and one can not guarantee that the results obtained are in fact a good approximation to a possible solution.

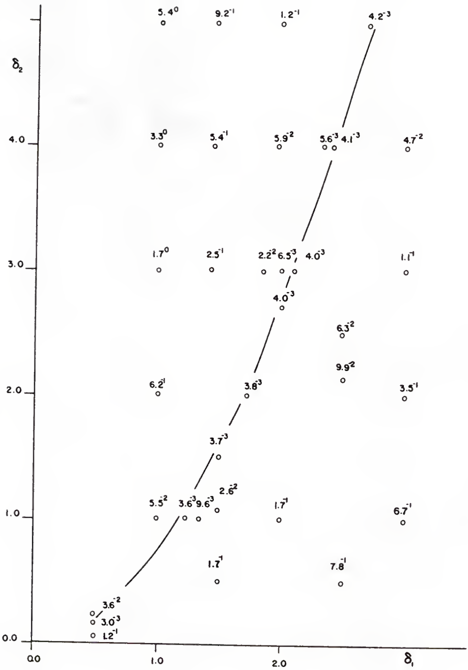

Figure 4.1: Mean quadratic error at the DFSBC.

### 4.3 Numerical Relationship between the Parameters

The results shown in the previous sections can be explained in view of equation (3.19)

$$\alpha\epsilon^2\,\frac{X_1^2 - X_0^2}{2}\left(\frac{\delta_2}{\delta_1^2} - \frac{\gamma_2}{X_0^2\,X_1^2}\psi_\eta^2\right) = 1.$$

First, let all parameters but $\delta_1$ and $\delta_2$ be held constant. Therefore, in order for the previous equation to be satisfied, a quadratic relationship should be expected between $\delta_1$ and $\delta_2$. Table (4.3) shows the computed values of the left hand side of that relationship for the cases being studied.

The relationship between $\psi_\eta$ and $\epsilon = kh$ is more significant because small variations in one parameter may cause large ones in the other. For instance, for $\gamma_2 = -.16$, $\delta_1 = .151$, $\delta_2 = 1.49$, equation (3.19) is satisfied when $\psi_\eta = .233$ and $\epsilon = .395$, as well as when $\psi_\eta = 2.05$ and $\epsilon = .378$. A change in 4% in $\epsilon$ may cause an increase of ten times in $\psi_\eta$.

### 4.4 Horizontal Velocity Profile

The velocity profiles were computed at crest and at trough, separating the flow in three components. First, a steady mean velocity, obtained by averaging the total velocity over one wave length. Below trough level, let it be represented as

$$U - c = \overline{-\psi_z} = -\frac{\epsilon}{\delta_1}\,\overline{X(x;\gamma_2)}\,Z(z;\delta_2).$$

In this expression, the effect of translating the coordinate system is included. Knowing the wave length, since the period of the wave with respect to the bottom can be chosen arbitrarily, the celerity can be determined. This will yield a different value for the current with respect to the (fixed) bottom, although the total velocity for an observer following the wave remains the same. The fact that, for cases 1 through 3, the mean current is larger at the bottom than at trough level is a consequence only of the choice of wave period. Basically, the shape of the current profile — and the distribution of vorticity — is not altered by adding a different (constant) value of wave celerity.

Subtracting the mean value presented above from the total velocity, the oscillatory component is obtained, which will be identified as the wave component. By the way it is defined, averaging this component over one wave length below trough level will yield a zero value and above trough level, will result in the mass flux induced by the wave. In all cases, the oscillatory component decreases with depth.

The results are shown in tables (4.4)–(4.13), which give, at several elevations below trough level, the mean current $U$, the oscillatory component $u'$, and the total velocity relative to a fixed observer $U + u'$, at crest and at trough, for the three theories being considered.

For each case, the current profile was adjusted to a straight line, i.e. constant vorticity, defined by the mean velocity at the bottom and the one at trough level. The SFWT was then used to compute the flow velocities and wave length. Except for Case 4, the values of vorticity are rather small; consequently the current is almost uniform over depth, and the SFWT is indeed more appropriate to use.

Cases 1, 2, and 2A, being in very shallow water, present a strong asymmetry between crest and trough. At the bottom, for instance, the ratio of values vary from three to eight times, and it tends to increase at higher elevations. The same is not observed for the present theory, where the difference is of the order of 10%, nor for the first order SFWT where the magnitudes must be equal.

## 4.5 Vorticity Distribution

Equation (3.29) expresses the dimensionless vorticity in terms of the stream function and the results are shown in tables (4.20)-(4.24). Except for cases 1 and 2A, the value of vorticity increases from zero at the bottom to a maximum value around mid-depth, and then decreases towards the free surface; at the bottom the vorticity is always equal to zero. This is in agreement with the definition of the vorticity distribution, qualitatively depicted in figure (3.5).

Table 4.4: Present theory velocities at different elevations below trough level: Case 1. Values in m/sec.

| elevation $z/h$ | total at crest | wave $u'\|_c$ | mean $U$ | wave $u'\|_t$ | total at trough |
|---|---|---|---|---|---|
| -0.4 | 6.671 | 1.520 | 5.151 | -1.636 | 3.515 |
| -0.5 | 6.682 | 1.514 | 5.168 | -1.629 | 3.539 |
| -0.6 | 6.693 | 1.508 | 5.184 | -1.623 | 3.561 |
| -0.7 | 6.702 | 1.503 | 5.199 | -1.618 | 3.581 |
| -0.8 | 6.710 | 1.499 | 5.211 | -1.613 | 3.598 |
| -0.9 | 6.716 | 1.496 | 5.220 | -1.610 | 3.610 |
| -1.0 | 6.719 | 1.494 | 5.224 | -1.608 | 3.616 |

Table 4.5: SFWT velocities at different elevations below trough level: Case 1. Values in m/sec.

| elevation $z/h$ | total at crest | wave $u'\|_c$ | mean $U$ | wave $u'\|_t$ | total at trough |
|---|---|---|---|---|---|
| -0.1 | 7.217 | 2.102 | 5.115 | -0.240 | 4.875 |
| -0.2 | 7.133 | 2.006 | 5.127 | -0.240 | 4.887 |
| -0.3 | 7.064 | 1.925 | 5.139 | -0.240 | 4.899 |
| -0.4 | 7.008 | 1.857 | 5.151 | -0.240 | 4.911 |
| -0.5 | 6.965 | 1.802 | 5.163 | -0.240 | 4.923 |
| -0.6 | 6.934 | 1.758 | 5.175 | -0.240 | 4.935 |
| -0.7 | 6.912 | 1.725 | 5.188 | -0.240 | 4.947 |
| -0.8 | 6.901 | 1.702 | 5.200 | -0.240 | 4.959 |
| -0.9 | 6.899 | 1.688 | 5.212 | -0.240 | 4.971 |
| -1.0 | 6.907 | 1.683 | 5.224 | -0.240 | 4.984 |

Table 4.6: SFWT (1) velocities at different elevations below trough level: Case 1. Values in m/sec.

| elevation $z/h$ | total at crest | wave $u'\|_c$ | mean $U$ | wave $u'\|_t$ | total at trough |
|---|---|---|---|---|---|
| -0.3 | 6.675 | 1.536 | 5.139 | -1.536 | 3.603 |
| -0.4 | 6.682 | 1.531 | 5.151 | -1.531 | 3.620 |
| -0.5 | 6.690 | 1.527 | 5.163 | -1.527 | 3.636 |
| -0.6 | 6.699 | 1.524 | 5.175 | -1.524 | 3.651 |
| -0.7 | 6.709 | 1.521 | 5.188 | -1.521 | 3.666 |
| -0.8 | 6.719 | 1.520 | 5.200 | -1.520 | 3.680 |
| -0.9 | 6.730 | 1.519 | 5.212 | -1.519 | 3.693 |
| -1.0 | 6.742 | 1.518 | 5.224 | -1.518 | 3.706 |

Table 4.7: Present theory velocities at different elevations below trough level: Case 2. Values in m/sec.

| elevation $z/h$ | total at crest | wave $u'\|_c$ | mean $U$ | wave $u'\|_t$ | total at trough |
|---|---|---|---|---|---|
| -0.3 | 7.996 | 2.496 | 5.500 | -2.636 | 2.864 |
| -0.4 | 8.052 | 2.478 | 5.574 | -2.616 | 2.958 |
| -0.5 | 8.109 | 2.458 | 5.652 | -2.595 | 3.056 |
| -0.6 | 8.168 | 2.438 | 5.730 | -2.574 | 3.156 |
| -0.7 | 8.224 | 2.419 | 5.805 | -2.554 | 3.251 |
| -0.8 | 8.274 | 2.401 | 5.872 | -2.536 | 3.336 |
| -0.9 | 8.313 | 2.388 | 5.925 | -2.522 | 3.403 |
| -1.0 | 8.331 | 2.382 | 5.950 | -2.515 | 3.434 |

Table 4.8: SFWT velocities at different elevations below trough level: Case 2. Values in m/sec.

| elevation $z/h$ | total at crest | wave $u'\|_c$ | mean $U$ | wave $u'\|_t$ | total at trough |
|---|---|---|---|---|---|
| -0.2 | 8.864 | 3.428 | 5.436 | -0.974 | 4.461 |
| -0.3 | 8.792 | 3.292 | 5.500 | -0.974 | 4.526 |
| -0.4 | 8.741 | 3.177 | 5.564 | -0.973 | 4.591 |
| -0.5 | 8.711 | 3.083 | 5.629 | -0.973 | 4.656 |
| -0.6 | 8.700 | 3.008 | 5.693 | -0.973 | 4.720 |
| -0.7 | 8.707 | 2.950 | 5.757 | -0.972 | 4.785 |
| -0.8 | 8.731 | 2.910 | 5.821 | -0.972 | 4.849 |
| -0.9 | 8.771 | 2.885 | 5.886 | -0.972 | 4.914 |
| -1.0 | 8.827 | 2.877 | 5.950 | -0.972 | 4.978 |

Table 4.9: SFWT (1) velocities at different elevations below trough level: Case 2. Values in m/sec.

| elevation $z/h$ | total at crest | wave $u'\|_c$ | mean $U$ | wave $u'\|_t$ | total at trough |
|---|---|---|---|---|---|
| -0.3 | 8.060 | 2.560 | 5.500 | -2.560 | 2.940 |
| -0.4 | 8.097 | 2.533 | 5.564 | -2.533 | 3.032 |
| -0.5 | 8.138 | 2.510 | 5.629 | -2.510 | 3.119 |
| -0.6 | 8.184 | 2.491 | 5.693 | -2.491 | 3.202 |
| -0.7 | 8.234 | 2.477 | 5.757 | -2.477 | 3.280 |
| -0.8 | 8.288 | 2.466 | 5.821 | -2.466 | 3.355 |
| -0.9 | 8.346 | 2.460 | 5.886 | -2.460 | 3.425 |
| -1.0 | 8.408 | 2.458 | 5.950 | -2.458 | 3.492 |

Table 4.10: Present theory velocities at different elevations below trough level: Case 2A. Values in m/sec.

| elevation $z/h$ | total at crest | wave $u'\|_c$ | mean $U$ | wave $u'\|_t$ | total at trough |
|---|---|---|---|---|---|
| -0.3 | 7.911 | 2.526 | 5.385 | -2.667 | 2.718 |
| -0.4 | 8.052 | 2.477 | 5.575 | -2.616 | 2.959 |
| -0.5 | 8.182 | 2.433 | 5.750 | -2.569 | 3.181 |
| -0.6 | 8.299 | 2.393 | 5.906 | -2.527 | 3.379 |
| -0.7 | 8.400 | 2.358 | 6.042 | -2.490 | 3.551 |
| -0.8 | 8.481 | 2.330 | 6.151 | -2.461 | 3.690 |
| -0.9 | 8.539 | 2.311 | 6.228 | -2.440 | 3.788 |
| -1.0 | 8.563 | 2.302 | 6.261 | -2.431 | 3.830 |

Table 4.11: SFWT velocities at different elevations below trough level: Case 2A. Values in m/sec.

| elevation $z/h$ | total at crest | wave $u'\|_c$ | mean $U$ | wave $u'\|_t$ | total at trough |
|---|---|---|---|---|---|
| -0.2 | 8.796 | 3.536 | 5.260 | -1.058 | 4.202 |
| -0.3 | 8.789 | 3.404 | 5.385 | -1.057 | 4.328 |
| -0.4 | 8.803 | 3.293 | 5.510 | -1.056 | 4.454 |
| -0.5 | 8.837 | 3.201 | 5.635 | -1.056 | 4.580 |
| -0.6 | 8.888 | 3.128 | 5.760 | -1.055 | 4.705 |
| -0.7 | 8.957 | 3.072 | 5.886 | -1.055 | 4.831 |
| -0.8 | 9.043 | 3.032 | 6.011 | -1.054 | 4.956 |
| -0.9 | 9.144 | 3.009 | 6.136 | -1.054 | 5.082 |
| -1.0 | 9.262 | 3.001 | 6.261 | -1.054 | 5.207 |

Table 4.12: SFWT (1) velocities at different elevations below trough level: Case 2A. Values in m/sec.

| elevation $z/h$ | total at crest | wave $u'\|_c$ | mean $U$ | wave $u'\|_t$ | total at trough |
|---|---|---|---|---|---|
| -0.3 | 8.027 | 2.642 | 5.385 | -2.642 | 2.743 |
| -0.4 | 8.124 | 2.614 | 5.510 | -2.614 | 2.896 |
| -0.5 | 8.225 | 2.590 | 5.635 | -2.590 | 3.045 |
| -0.6 | 8.331 | 2.571 | 5.760 | -2.571 | 3.190 |
| -0.7 | 8.442 | 2.556 | 5.886 | -2.556 | 3.330 |
| -0.8 | 8.556 | 2.545 | 6.011 | -2.545 | 3.465 |
| -0.9 | 8.675 | 2.539 | 6.136 | -2.539 | 3.597 |
| -1.0 | 8.798 | 2.537 | 6.261 | -2.537 | 3.724 |

Table 4.13: Present theory velocities at different elevations below trough level: Case 3. Values in m/sec.

| elevation $z/h$ | total at crest | wave $u'\|_c$ | mean $U$ | wave $u'\|_t$ | total at trough |
|---|---|---|---|---|---|
| -0.2 | -1.274 | 0.971 | -2.245 | -1.007 | -3.251 |
| -0.3 | -1.183 | 0.954 | -2.137 | -0.989 | -3.126 |
| -0.4 | -1.070 | 0.933 | -2.003 | -0.968 | -2.970 |
| -0.5 | -0.940 | 0.909 | -1.849 | -0.943 | -2.793 |
| -0.6 | -0.802 | 0.884 | -1.686 | -0.917 | -2.604 |
| -0.7 | -0.665 | 0.859 | -1.524 | -0.891 | -2.415 |
| -0.8 | -0.539 | 0.836 | -1.375 | -0.867 | -2.243 |
| -0.9 | -0.439 | 0.818 | -1.257 | -0.848 | -2.105 |
| -1.0 | -0.391 | 0.809 | -1.200 | -0.839 | -2.039 |

Table 4.14: SFWT velocities at different elevations below trough level: Case 3. Values in m/sec.

| elevation $z/h$ | total at crest | wave $u'\|_c$ | mean $U$ | wave $u'\|_t$ | total at trough |
|---|---|---|---|---|---|
| -0.2 | -1.121 | 1.124 | -2.245 | -0.878 | -3.123 |
| -0.3 | -1.053 | 1.061 | -2.114 | -0.847 | -2.962 |
| -0.4 | -0.976 | 1.008 | -1.984 | -0.821 | -2.804 |
| -0.5 | -0.889 | 0.964 | -1.853 | -0.798 | -2.651 |
| -0.6 | -0.794 | 0.929 | -1.723 | -0.780 | -2.502 |
| -0.7 | -0.690 | 0.902 | -1.592 | -0.766 | -2.357 |
| -0.8 | -0.579 | 0.883 | -1.461 | -0.755 | -2.217 |
| -0.9 | -0.459 | 0.871 | -1.331 | -0.749 | -2.080 |
| -1.0 | -0.332 | 0.868 | -1.200 | -0.747 | -1.947 |

Table 4.15: SFWT (1) velocities at different elevations below trough level: Case 3. Values in m/sec.

| elevation $z/h$ | total at crest | wave $u'\|_c$ | mean $U$ | wave $u'\|_t$ | total at trough |
|---|---|---|---|---|---|
| -0.2 | -1.213 | 1.032 | -2.245 | -1.032 | -3.277 |
| -0.3 | -1.132 | 0.982 | -2.114 | -0.982 | -3.096 |
| -0.4 | -1.044 | 0.940 | -1.984 | -0.940 | -2.924 |
| -0.5 | -0.949 | 0.905 | -1.853 | -0.905 | -2.758 |
| -0.6 | -0.846 | 0.876 | -1.723 | -0.876 | -2.599 |
| -0.7 | -0.738 | 0.854 | -1.592 | -0.854 | -2.446 |
| -0.8 | -0.623 | 0.839 | -1.461 | -0.839 | -2.300 |
| -0.9 | -0.501 | 0.829 | -1.331 | -0.829 | -2.160 |
| -1.0 | -0.374 | 0.826 | -1.200 | -0.826 | -2.026 |

Table 4.16: Present theory velocities at different elevations below trough level: Case 4. Values in m/sec.

| elevation $z/h$ | total at crest | wave $u'\|_c$ | mean $U$ | wave $u'\|_t$ | total at trough |
|---|---|---|---|---|---|
| -0.1 | -4.588 | 0.916 | -5.505 | -0.941 | -6.446 |
| -0.2 | -4.268 | 0.881 | -5.149 | -0.905 | -6.055 |
| -0.3 | -3.789 | 0.829 | -4.617 | -0.851 | -5.469 |
| -0.4 | -3.199 | 0.764 | -3.964 | -0.785 | -4.749 |
| -0.5 | -2.551 | 0.693 | -3.244 | -0.712 | -3.956 |
| -0.6 | -1.892 | 0.621 | -2.514 | -0.638 | -3.152 |
| -0.7 | -1.271 | 0.553 | -1.824 | -0.568 | -2.392 |
| -0.8 | -0.732 | 0.494 | -1.226 | -0.508 | -1.733 |
| -0.9 | -0.328 | 0.450 | -0.777 | -0.462 | -1.239 |
| -1.0 | -0.143 | 0.430 | -0.572 | -0.441 | -1.013 |

Table 4.17: SFWT velocities at different elevations below trough level: Case 4. Values in m/sec.

| elevation $z/h$ | total at crest | wave $u'\|_c$ | mean $U$ | wave $u'\|_t$ | total at trough |
|---|---|---|---|---|---|
| -0.1 | -4.428 | 1.077 | -5.505 | -1.095 | -6.600 |
| -0.2 | -3.989 | 0.968 | -4.957 | -0.982 | -5.939 |
| -0.3 | -3.533 | 0.876 | -4.409 | -0.886 | -5.295 |
| -0.4 | -3.062 | 0.799 | -3.861 | -0.807 | -4.668 |
| -0.5 | -2.577 | 0.736 | -3.313 | -0.742 | -4.055 |
| -0.6 | -2.079 | 0.685 | -2.764 | -0.690 | -3.455 |
| -0.7 | -1.569 | 0.647 | -2.216 | -0.651 | -2.868 |
| -0.8 | -1.048 | 0.620 | -1.668 | -0.624 | -2.292 |
| -0.9 | -0.516 | 0.604 | -1.120 | -0.608 | -1.728 |
| -1.0 | 0.027 | 0.599 | -0.572 | -0.602 | -1.174 |

Table 4.18: SFWT (1) velocities at different elevations below trough level: Case 4. Values in m/sec.

| elevation $z/h$ | total at crest | wave $u'\|_c$ | mean $U$ | wave $u'\|_t$ | total at trough |
|---|---|---|---|---|---|
| -0.1 | -4.420 | 1.085 | -5.505 | -1.085 | -6.590 |
| -0.2 | -3.983 | 0.974 | -4.957 | -0.974 | -5.931 |
| -0.3 | -3.529 | 0.880 | -4.409 | -0.880 | -5.289 |
| -0.4 | -3.059 | 0.802 | -3.861 | -0.802 | -4.662 |
| -0.5 | -2.575 | 0.738 | -3.313 | -0.738 | -4.050 |
| -0.6 | -2.078 | 0.687 | -2.764 | -0.687 | -3.451 |
| -0.7 | -1.568 | 0.648 | -2.216 | -0.648 | -2.864 |
| -0.8 | -1.047 | 0.621 | -1.668 | -0.621 | -2.289 |
| -0.9 | -0.515 | 0.605 | -1.120 | -0.605 | -1.725 |
| -1.0 | 0.028 | 0.600 | -0.572 | -0.600 | -1.172 |

Also listed on those tables are the contributions from the horizontal gradient of the vertical velocity and the vertical gradient of the horizontal velocity, computed at crest and at trough. As pointed out in section 3.4.1, they are not equal to the total vorticity and, locally, the gradient of vertical velocity may be as large as one third of the total vorticity. This usually happens under the crest.

It is more significant, though, to compare the average values of those gradients. If the contribution of the mean current is subtracted from $\omega$, the remainder is the vorticity associated with the oscillatory motion. For the cases being considered, the order of magnitude of the vorticity in the current can be estimated by the gradient between the mean velocity at trough level and at the bottom. Subtracting these values from the value of total vorticity, the maximum wave motion contribution ranges from 20% to 45% of the total vorticity. Values are shown in table (4.25).

### 4.6 Free Surface Elevation and Wave Length

As shown in table (4.19), the wave length predicted by the present theory is within 10% of the value given by the SFWT. However, the free surface profile shows considerable differences. While the SFWT predicts a sharp crest and flat trough, which is particularly true for the conditions corresponding to $\gamma_2 = -.14$, the present theory gives a more symmetric (say, "linear") shape of the free surface. One explanation is again the difference between the DFSBC error for both theories.

Figures (4.2) and (4.3) show the profiles scaled by the total wave height. For the Stream Function cases, the mean water level is zero and the difference in elevation between trough and crest is set equal to 1. However, the zero mean water level as well as the nondimensional unity wave height were only accomplished approximately for the present theory, and this explains the apparent uniform translation shown in case 1; in general, the profile fits almost exactly the one given by SFWT (1).

Table 4.19: Wave length: comparison with Stream Function Theory ($L_{\mathrm{SF}}$), first order SFWT ($L_{\mathrm{I}}$), and Linear Wave Theory ($L_{\mathrm{L}}$).

| Case | $L$ (m) | $L_{\mathrm{SF}}$ (m) | $L_{\mathrm{I}}$ (m) | $L_{\mathrm{L}}$ (m) |
|---|---|---|---|---|
| 1 | 56.93 | 63.07 | 57.58 | 57.34 |
| 2 | 152.9 | 163.9 | 156.1 | 152.6 |
| 2A | 152.9 | 163.6 | 153.4 | 152.6 |
| 3 | 32.28 | 32.89 | 32.15 | 54.78 |
| 4 | 45.35 | 44.71 | 57.52 | 51.47 |

Table 4.20: Dimensionless vorticity under crest and trough: Case 1.

| $\psi/\psi_\eta$ | $\omega$ | $\overline{u_z}$ | $\overline{\epsilon^2 w_x}$ | $u_z\|_{\mathrm{c}}$ | $\epsilon^2 w_x\|_{\mathrm{c}}$ | $u_z\|_{\mathrm{t}}$ | $\epsilon^2 w_x\|_{\mathrm{t}}$ |
|---|---|---|---|---|---|---|---|
| 1.0 | -0.0611 | -0.0569 | 0.0043 | -0.0321 | 0.0290 | -0.0789 | -0.0177 |
| 0.9 | -0.0609 | -0.0571 | 0.0038 | -0.0348 | 0.0261 | -0.0769 | -0.0160 |
| 0.8 | -0.0600 | -0.0566 | 0.0034 | -0.0368 | 0.0232 | -0.0742 | -0.0142 |
| 0.7 | -0.0583 | -0.0553 | 0.0030 | -0.0380 | 0.0203 | -0.0707 | -0.0124 |
| 0.6 | -0.0557 | -0.0532 | 0.0026 | -0.0383 | 0.0174 | -0.0664 | -0.0106 |
| 0.5 | -0.0521 | -0.0500 | 0.0021 | -0.0376 | 0.0145 | -0.0610 | -0.0089 |
| 0.4 | -0.0473 | -0.0455 | 0.0017 | -0.0356 | 0.0116 | -0.0543 | -0.0071 |
| 0.3 | -0.0408 | -0.0395 | 0.0013 | -0.0321 | 0.0087 | -0.0461 | -0.0053 |
| 0.2 | -0.0323 | -0.0314 | 0.0009 | -0.0264 | 0.0058 | -0.0358 | -0.0035 |
| 0.1 | -0.0204 | -0.0200 | 0.0004 | -0.0175 | 0.0029 | -0.0222 | -0.0018 |

Table 4.21: Dimensionless vorticity under crest and trough: Case 2.

| $\psi/\psi_\eta$ | $\omega$ | $\overline{u_z}$ | $\overline{\epsilon^2 w_x}$ | $u_z\|_{\mathrm{c}}$ | $\epsilon^2 w_x\|_{\mathrm{c}}$ | $u_z\|_{\mathrm{t}}$ | $\epsilon^2 w_x\|_{\mathrm{t}}$ |
|---|---|---|---|---|---|---|---|
| 1.0 | -0.0938 | -0.0827 | 0.0111 | 0.0034 | 0.0971 | -0.1621 | -0.0683 |
| 0.9 | -0.1138 | -0.1039 | 0.0100 | -0.0264 | 0.0874 | -0.1753 | -0.0615 |
| 0.8 | -0.1304 | -0.1216 | 0.0089 | -0.0527 | 0.0777 | -0.1851 | -0.0546 |
| 0.7 | -0.1431 | -0.1354 | 0.0077 | -0.0751 | 0.0680 | -0.1910 | -0.0478 |
| 0.6 | -0.1514 | -0.1448 | 0.0066 | -0.0931 | 0.0583 | -0.1924 | -0.0410 |
| 0.5 | -0.1545 | -0.1489 | 0.0055 | -0.1059 | 0.0486 | -0.1886 | -0.0341 |
| 0.4 | -0.1513 | -0.1469 | 0.0044 | -0.1124 | 0.0389 | -0.1786 | -0.0273 |
| 0.3 | -0.1403 | -0.1369 | 0.0033 | -0.1111 | 0.0291 | -0.1607 | -0.0205 |
| 0.2 | -0.1187 | -0.1165 | 0.0022 | -0.0993 | 0.0194 | -0.1323 | -0.0137 |
| 0.1 | -0.0809 | -0.0798 | 0.0011 | -0.0711 | 0.0097 | -0.0877 | -0.0068 |

Table 4.22: Dimensionless vorticity under crest and trough: Case 2A.

| $\psi/\psi_\eta$ | $\omega$ | $\overline{u_z}$ | $\overline{\epsilon^2 w_x}$ | $u_z\|_c$ | $\epsilon^2 w_x\|_c$ | $u_z\|_t$ | $\epsilon^2 w_x\|_t$ |
|---|---|---|---|---|---|---|---|
| 1.0 | -0.4348 | -0.4238 | 0.0111 | -0.3377 | 0.0971 | -0.5031 | -0.0683 |
| 0.9 | -0.4208 | -0.4108 | 0.0100 | -0.3334 | 0.0874 | -0.4822 | -0.0615 |
| 0.8 | -0.4033 | -0.3944 | 0.0089 | -0.3256 | 0.0777 | -0.4579 | -0.0546 |
| 0.7 | -0.3819 | -0.3741 | 0.0077 | -0.3139 | 0.0680 | -0.4297 | -0.0478 |
| 0.6 | -0.3560 | -0.3494 | 0.0066 | -0.2978 | 0.0583 | -0.3970 | -0.0410 |
| 0.5 | -0.3250 | -0.3195 | 0.0055 | -0.2764 | 0.0486 | -0.3592 | -0.0341 |
| 0.4 | -0.2877 | -0.2833 | 0.0044 | -0.2489 | 0.0389 | -0.3150 | -0.0273 |
| 0.3 | -0.2426 | -0.2393 | 0.0033 | -0.2134 | 0.0291 | -0.2631 | -0.0205 |
| 0.2 | -0.1869 | -0.1847 | 0.0022 | -0.1675 | 0.0194 | -0.2006 | -0.0137 |
| 0.1 | -0.1150 | -0.1139 | 0.0011 | -0.1053 | 0.0097 | -0.1218 | -0.0068 |

Table 4.23: Dimensionless vorticity under crest and trough: Case 3.

| $\psi/\psi_\eta$ | $\omega$ | $\overline{u_z}$ | $\overline{\epsilon^2 w_x}$ | $u_z\|_c$ | $\epsilon^2 w_x\|_c$ | $u_z\|_t$ | $\epsilon^2 w_x\|_t$ |
|---|---|---|---|---|---|---|---|
| 1.0 | -0.1045 | -0.0752 | 0.0292 | 0.2864 | 0.3909 | -0.4212 | -0.3167 |
| 0.9 | -0.3060 | -0.2797 | 0.0263 | 0.0458 | 0.3518 | -0.5911 | -0.2851 |
| 0.8 | -0.4827 | -0.4593 | 0.0234 | -0.1699 | 0.3127 | -0.7360 | -0.2534 |
| 0.7 | -0.6313 | -0.6108 | 0.0205 | -0.3577 | 0.2736 | -0.8530 | -0.2217 |
| 0.6 | -0.7479 | -0.7303 | 0.0175 | -0.5133 | 0.2345 | -0.9379 | -0.1900 |
| 0.5 | -0.8270 | -0.8124 | 0.0146 | -0.6316 | 0.1954 | -0.9854 | -0.1584 |
| 0.4 | -0.8611 | -0.8494 | 0.0117 | -0.7048 | 0.1564 | -0.9878 | -0.1267 |
| 0.3 | -0.8388 | -0.8300 | 0.0088 | -0.7215 | 0.1173 | -0.9338 | -0.0950 |
| 0.2 | -0.7405 | -0.7346 | 0.0058 | -0.6623 | 0.0782 | -0.8038 | -0.0633 |
| 0.1 | -0.5252 | -0.5223 | 0.0029 | -0.4861 | 0.0391 | -0.5569 | -0.0317 |

Table 4.24: Dimensionless vorticity under crest and trough: Case 4.

| $\psi/\psi_\eta$ | $\omega$ | $\overline{u_z}$ | $\overline{\epsilon^2 w_x}$ | $u_z\|_c$ | $\epsilon^2 w_x\|_c$ | $u_z\|_t$ | $\epsilon^2 w_x\|_t$ |
|---|---|---|---|---|---|---|---|
| 1.0 | -0.0916 | -0.0243 | 0.0673 | 1.2265 | 1.3181 | -1.2450 | -1.1534 |
| 0.9 | -1.2512 | -1.1906 | 0.0606 | -0.0649 | 1.1863 | -2.2893 | -1.0380 |
| 0.8 | -2.2736 | -2.2198 | 0.0539 | -1.2191 | 1.0545 | -3.1963 | -0.9227 |
| 0.7 | -3.1415 | -3.0944 | 0.0471 | -2.2189 | 0.9227 | -3.9489 | -0.8074 |
| 0.6 | -3.8328 | -3.7924 | 0.0404 | -3.0419 | 0.7909 | -4.5248 | -0.6920 |
| 0.5 | -4.3176 | -4.2840 | 0.0337 | -3.6585 | 0.6591 | -4.8943 | -0.5767 |
| 0.4 | -4.5543 | -4.5273 | 0.0269 | -4.0270 | 0.5272 | -5.0156 | -0.4614 |
| 0.3 | -4.4795 | -4.4593 | 0.0202 | -4.0840 | 0.3954 | -4.8255 | -0.3460 |
| 0.2 | -3.9859 | -3.9724 | 0.0135 | -3.7222 | 0.2636 | -4.2165 | -0.2307 |
| 0.1 | -2.8473 | -2.8406 | 0.0067 | -2.7155 | 0.1318 | -2.9626 | -0.1153 |

Table 4.25: Estimate of the wave motion contribution to the total vorticity. $\omega_0$ is the dimensionless value of vorticity used in the SFWT.

| Case | $\omega_0$ | $\omega_{\max} - \omega_0$ | percentage |
|---|---|---|---|
| 1 | -0.03781 | -0.02329 | -38% |
| 2 | -0.1239 | -0.0306 | -20% |
| 2A | -0.2413 | -0.1935 | -45% |
| 3 | -0.6797 | -0.1814 | -21% |
| 4 | -3.396 | -1.158 | -25% |

## 4.7 Pressure

The dynamic pressure, given by equation (3.37), is computed under the crest and under the trough, at fixed elevations. For the SFWT the expression for dynamic pressure is easily obtained because the vorticity is constant. Hence, the integral in equation (3.35) becomes simply the vorticity times the total discharge between the given elevation and the free surface.

The values shown in tables (4.26) – (4.30) are made dimensionless after dividing the pressure by $\rho g H/2$. The pressure is computed up to the highest elevation below trough level allowed by the theory chosen. For this reason, the tables show values at higher elevations for the SFWT, which exhibits a strong asymetry of free surface profile.

In agreement with what has been seen with other properties, in all five cases, the pressure is of approximately the same magnitude at crest and at trough, another characteristic of linear waves. As an example, figure (4.4) shows the dimensionless dynamic pressure at the bottom, along half wave length, for Case 2.

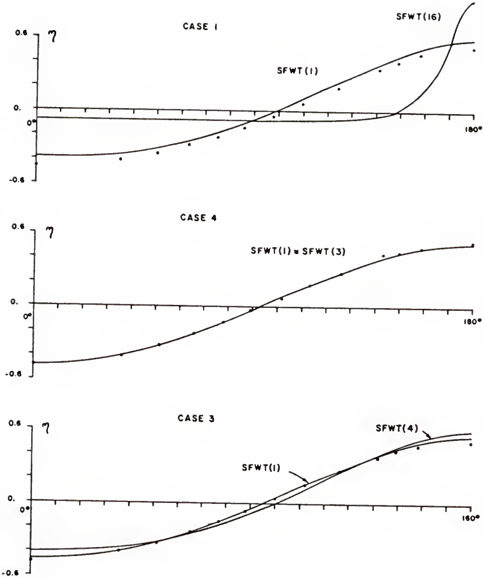

Figure 4.2: Free surface elevation: Cases 1, 3, and 4. ( — ) SFWT, ( • ) present theory.

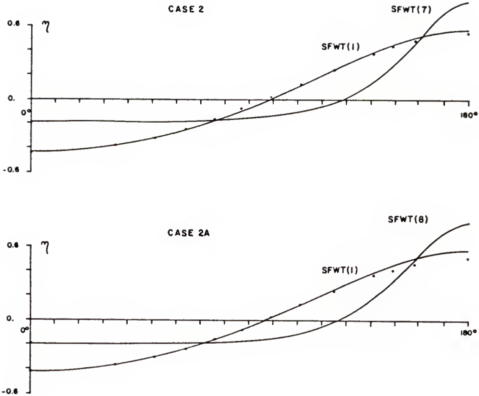

Figure 4.3: Free surface elevation: Cases 2 and 2A. ( — ) SFWT, ( • ) present theory.

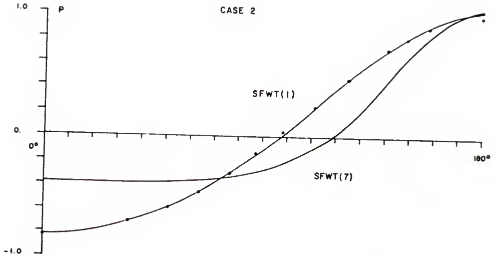

Figure 4.4: Dimensionless dynamic pressure at the bottom: Case 2.

Table 4.26: Dimensionless dynamic pressure distribution at crest and at trough: Case 1

| | SFWT | | SFWT (1) | | Eq.(3.37) | |
|---|---|---|---|---|---|---|
| $z/h$ | crest | trough | crest | trough | crest | trough |
| 0.0 | 1.3271 | – | 1.1611 | – | 1.052 | – |
| -0.1 | 1.2754 | -0.1615 | 1.1582 | – | 1.050 | – |
| -0.2 | 1.2303 | -0.1617 | 1.1557 | – | 1.047 | – |
| -0.3 | 1.1914 | -0.1618 | 1.1534 | -0.8232 | 1.045 | – |
| -0.4 | 1.1585 | -0.1619 | 1.1515 | -0.8192 | 1.044 | -0.924 |
| -0.5 | 1.1312 | -0.1619 | 1.1499 | -0.8159 | 1.042 | -0.920 |
| -0.6 | 1.1093 | -0.1619 | 1.1486 | -0.8132 | 1.041 | -0.916 |
| -0.7 | 1.0925 | -0.1620 | 1.1475 | -0.8111 | 1.040 | -0.914 |
| -0.8 | 1.0807 | -0.1620 | 1.1468 | -0.8096 | 1.040 | -0.912 |
| -0.9 | 1.0737 | -0.1620 | 1.1464 | -0.8087 | 1.039 | -0.911 |
| -1.0 | 1.0713 | -0.1620 | 1.1462 | -0.8084 | 1.039 | -0.911 |

Table 4.27: Dimensionless dynamic pressure distribution at crest and at trough: Case 2

| | SFWT | | SFWT (1) | | Eq.(3.37) | |
|---|---|---|---|---|---|---|
| $z/h$ | crest | trough | crest | trough | crest | trough |
| 0.0 | 1.3035 | – | 1.0903 | – | 1.057 | – |
| -0.1 | 1.2497 | – | 1.0788 | – | 1.047 | – |
| -0.2 | 1.2029 | -0.3831 | 1.0686 | – | 1.037 | – |
| -0.3 | 1.1627 | -0.3829 | 1.0597 | -0.8569 | 1.029 | -0.876 |
| -0.4 | 1.1286 | -0.3827 | 1.0520 | -0.8438 | 1.022 | -0.861 |
| -0.5 | 1.1005 | -0.3825 | 1.0456 | -0.8329 | 1.016 | -0.849 |
| -0.6 | 1.0780 | -0.3823 | 1.0404 | -0.8240 | 1.011 | -0.839 |
| -0.7 | 1.0607 | -0.3822 | 1.0364 | -0.8172 | 1.007 | -0.832 |
| -0.8 | 1.0486 | -0.3821 | 1.0335 | -0.8124 | 1.005 | -0.827 |
| -0.9 | 1.0415 | -0.3821 | 1.0318 | -0.8095 | 1.003 | -0.823 |
| -1.0 | 1.0391 | -0.3821 | 1.0313 | -0.8086 | 1.003 | -0.822 |

Table 4.28: Dimensionless dynamic pressure distribution at crest and at trough: Case 2A

| $z/h$ | SFWT | | SFWT (1) | | Eq.(3.37) | |
|---|---|---|---|---|---|---|
| | crest | trough | crest | trough | crest | trough |
| 0.0 | 1.2933 | – | 1.0837 | – | 0.979 | – |
| -0.1 | 1.2409 | – | 1.0715 | – | 0.968 | – |
| -0.2 | 1.1955 | -0.4018 | 1.0608 | – | 0.959 | – |
| -0.3 | 1.1566 | -0.4014 | 1.0515 | -0.8602 | 0.950 | -0.832 |
| -0.4 | 1.1239 | -0.4011 | 1.0436 | -0.8466 | 0.943 | -0.818 |
| -0.5 | 1.0970 | -0.4008 | 1.0370 | -0.8352 | 0.938 | -0.806 |
| -0.6 | 1.0756 | -0.4006 | 1.0317 | -0.8260 | 0.933 | -0.797 |
| -0.7 | 1.0594 | -0.4004 | 1.0276 | -0.8190 | 0.930 | -0.790 |
| -0.8 | 1.0480 | -0.4003 | 1.0248 | -0.8140 | 0.927 | -0.785 |
| -0.9 | 1.0413 | -0.4002 | 1.0231 | -0.8111 | 0.926 | -0.782 |
| -1.0 | 1.0391 | -0.4002 | 1.0226 | -0.8101 | 0.925 | -0.781 |

Table 4.29: Dimensionless dynamic pressure distribution at crest and at trough: Case 3

| $z/h$ | SFWT | | SFWT (1) | | Eq.(3.37) | |
|---|---|---|---|---|---|---|
| | crest | trough | crest | trough | crest | trough |
| 0.0 | 1.0312 | – | 0.9793 | – | 0.940 | – |
| -0.1 | 0.9594 | – | 0.9241 | – | 0.888 | – |
| -0.2 | 0.8979 | -0.7858 | 0.8764 | -0.8740 | 0.842 | -0.918 |
| -0.3 | 0.8461 | -0.7514 | 0.8357 | -0.8175 | 0.803 | -0.858 |
| -0.4 | 0.8030 | -0.7221 | 0.8016 | -0.7706 | 0.770 | -0.808 |
| -0.5 | 0.7679 | -0.6979 | 0.7737 | -0.7324 | 0.743 | -0.767 |
| -0.6 | 0.7403 | -0.6784 | 0.7516 | -0.7023 | 0.722 | -0.735 |
| -0.7 | 0.7196 | -0.6636 | 0.7349 | -0.6796 | 0.706 | -0.711 |
| -0.8 | 0.7054 | -0.6532 | 0.7234 | -0.6639 | 0.696 | -0.694 |
| -0.9 | 0.6971 | -0.6471 | 0.7167 | -0.6548 | 0.689 | -0.685 |
| -1.0 | 0.6944 | -0.6451 | 0.7145 | -0.6518 | 0.687 | -0.682 |

Table 4.30: Dimensionless dynamic pressure distribution at crest and at trough: Case 4

|  | SFWT |  | SFWT (1) |  | Eq.(3.37) |  |
|---|---|---|---|---|---|---|
| $z/h$ | crest | trough | crest | trough | crest | trough |
| 0.0 | 0.9176 | – | 0.9192 | – | 0.902 | – |
| -0.1 | 0.7812 | -0.9104 | 0.7798 | -0.9089 | 0.730 | -0.907 |
| -0.2 | 0.6699 | -0.7686 | 0.6664 | -0.7695 | 0.587 | -0.719 |
| -0.3 | 0.5804 | -0.6561 | 0.5754 | -0.6588 | 0.472 | -0.569 |
| -0.4 | 0.5097 | -0.5682 | 0.5036 | -0.5721 | 0.384 | -0.455 |
| -0.5 | 0.4552 | -0.5008 | 0.4484 | -0.5058 | 0.320 | -0.371 |
| -0.6 | 0.4146 | -0.4509 | 0.4073 | -0.4565 | 0.276 | -0.313 |
| -0.7 | 0.3858 | -0.4155 | 0.3783 | -0.4216 | 0.246 | -0.274 |
| -0.8 | 0.3672 | -0.3926 | 0.3595 | -0.3989 | 0.229 | -0.251 |
| -0.9 | 0.3571 | -0.3800 | 0.3493 | -0.3864 | 0.220 | -0.239 |
| -1.0 | 0.3540 | -0.3761 | 0.3462 | -0.3826 | 0.217 | -0.236 |

# CHAPTER 5
# SUMMARY OF RESULTS

The theory presented consists of a formal solution of the vorticity equation in two dimensions, which is periodic in space and valid for inviscid fluids. Consequently, it can be used for modelling waves on a rotational flow, as long as the profile of the current is described by a particular function, referenced in this work as $lsc(z; \delta_2)$.

Rigorous proof of existence of such solution satisfying the usual boundary conditions for free surface flows has not been found. However, there is numerical evidence of the validity of the theory in the sense that it was possible to minimize the mean square error on the dynamic free surface boundary condition.

The results were compared with the Stream Function Wave Theory developed by Dalrymple (1973) for waves on a constant shear current: both first order and higher order approximations were used. As a rule, the agreement between the first order approximation of the SFWT and the present theory was stronger than with the higher order, in accordance with the comparable values for the root mean square error.

The wave length and profiles showed a better agreement with linear waves, particularly regarding the shape of the profile, which is more symmetric instead of having peaked crests and flat troughs. The values for wave length differed by less than 3% from the first order SFWT, although the difference could be as high as 13% for the higher order theory.

The values of dynamic pressure did not show the strong asymmetry between trough and level as found in the Stream Function, which can be as much as six times higher at the crest. However, comparing with the first order Stream Function, the agreement was usually within 10%, and the values were more symmetric. As expected, the dynamic influence of the waves decrease with depth.

Regarding the velocity field, only values at crest and at trough were computed. For the cases studied, the present theory has approximately symmetric values between crest and trough throughout the water column, again in better agreement with the first order theory.

Although an attempt was made to extend this theory to deep water, all numerical results converged to shallow or intermediate water depth solutions. This happens because, given the form of the solution and its dependency on the vertical coordinate, the stream function would have to be an oscillatory function throughout the water column, i.e. between the free surface and bottom; further, there is no solution which would vanish at infinity, corresponding to a finite mass transport.

In the formulation of the general problem of waves in arbitrary current in terms of the stream function, one has to have a good description of the vorticity field. It is shown that, for the present theory, the contribution of the oscillatory motion to the total value of vorticity may range from 20% to 45% at the elevation where the maximum value of vorticity occurs. This means that the horizontal gradient of the vertical velocity may play a significant role in the distribution of vorticity. Therefore, the vorticity field may be underestimated if only the vertical gradient of the horizontal velocity is considered.

# CHAPTER 6
# RECOMMENDATIONS

The present theory needs to be further studied regarding its mathematical properties, especially with the purpose of establishing relations between the theoretical parameters and physical quantities. Also, if it is to be used for practical engineering purposes, the functions $lcc-$ and $lsc-$ would need to be readily accessible, being displayed in tables or series expansions. However, the major question remains, whether such a solution corresponds to a possible flow in nature. For the purpose of comparison with other rotational theories, the one developed by Dalrymple and Cox (1976) would seem to be more appropriate and the next logical step.

Due to the anlytical nature of the present theory and its simple algebraic expression, it is possible to derive in closed form several quantities of practical interest. Therefore, this theory may be used to obtain some qualitative information about the influence of vorticity on the propagation of waves.

The scaling adopted implicitly assumed shallow water approximation, and the results were compatible with this assumption. However, with minor modifications in the present development, a different scaling could be used leading to solutions valid in deeper water depths.

Among the theoretical aspects to be further investigated not only for the present theory but also for the general case of wave-current interaction, two points are of extreme interest. One concerns the stability of such flows since it has been proven in the literature (e.g. Yih (1972)) that the shape of the current profile determines whether the waves are stable. Another point is the study of three dimensional effects, which is more realistic for engineering applications. In three dimensions, the presence of the vortex stretching mechanism, which is absent in two dimensions, introduces a total different view of the problem in terms of vorticity transport.

For two dimensional motions, as a natural generalization of the method applied for the Stream Function Wave Theory, one might consider a formal solution,

$$\hat{\psi}(\hat{x},\hat{z}) \;=\; U(\hat{z}) \;+\; \sum_{n=1}^{N} X_n \sinh\left[(\gamma_n(k)(h+\hat{z})\right] \cos nk\hat{x},$$

where the function $U(\hat{z})$ would be arbitrary, and then apply the same methodology. In both cases studied by Dalrymple and by Dalrymple and Cox, the governing equations were linear and, as a consequence, the principle of superposition was valid. This is not true in general for arbitrary flows. If the above expression is substituted into the vorticity equation, and a proper ordering of terms is selected, it may be possible to obtain a hierarchy of differential equations which could be solved numerically. However, the resulting system and the conditions which the coefficients must satisfy are algebraically difficult to interpret and solve.

Any theory, however, would need to be verified experimentally. Towards a better understanding of the superposition of waves to a general rotational current, there is a need for more measurements as well as development of new techniques. The present methods, especially if only one component of velocity is observed, are totally unsatisfactory.

# APPENDIX A
# SEPARABLE SOLUTIONS OF VORTICITY EQUATION

## A.1 Qualitative description of the solutions

For steady irrotational flows, the vorticity equation becomes the Laplace equation in terms of the stream function. In general, however, for steady flows the conservation of vorticity is expressed as a third order, non linear partial differential equation in terms of the stream function:

$$\psi_z \nabla^2 \psi_x \; - \; \psi_x \nabla^2 \psi_z \; = \; 0. \tag{A.1}$$

In this form, which is also valid for the irrotational case, the application of the method of separation of variables is straightforward.

Assuming

$$\psi(x, z) \; = \; X(x)\, Z(z), \tag{A.2}$$

and substituting into the governing equation (A.1), two differential equations are obtained, one in $x$, one in $z$:

$$\frac{Z\,Z''' \; - \; Z'\,Z''}{Z\,Z'} \; = \; \frac{X\,X''' \; - \; X'\,X''}{X\,X'} \; = \; \text{constant}. \tag{A.3}$$

Depending on the value of the separation constant, different solutions are obtained. Their qualitative description is studied based on the phase plane trajectories, which can also be used to actually compute the values of the functions. It should be noted that both equations, for $X(x)$ and for $Z(z)$, are identical and, from now on, $Y$ will be considered as a general variable, except where reference to the specific function become necessary to avoid confusion. Each case will be studied separately.

### A.1.1 Case A: constant=0

This case yields the "exponential type" solutions obtained from the Laplace equation. The differential equation reduces to

$$\frac{Y'''}{Y''} = \frac{Y'}{Y} \Rightarrow Y'' + c_1 Y = 0 \tag{A.4}$$

which admits the following solutions:

$$Y(y) = \begin{cases} \alpha + \beta y & , c_1 = 0 & (A.5a) \\ \alpha\cos(\sqrt{c_1}\, y) + \beta\sin(\sqrt{c_1}\, y) & , c_1 > 0 & (A.5b) \\ \alpha\cosh(\sqrt{|c_1|}\, y) + \beta\sinh(\sqrt{|c_1|}\, y) & , c_1 < 0 & (A.5c) \end{cases}$$

For the first case, the trajectories in the phase plane are horizontal lines, because $Y'$ is always constant. For the second case, the trajectories are ellipses:

$$Y'^{\,2} + c_1 Y^{\,2} = c_1(\alpha^2 + \beta^2),$$

and all solutions are periodic. For the third case, the trajectories are hyperbolas given by the equation:

$$Y'^{\,2} - c_1 Y^{\,2} = c_1(\beta^2 - \alpha^2).$$

Because the differential equations for $X$ and $Z$ are uncoupled, the constant $c_1$ may actually assume different values, say $c_1$ for $X$ and $d_1$ for $Z$. The vorticity will then be given as

$$\omega = -\nabla^2\psi = (c_1 + d_1)\psi. \tag{A.6}$$

This is the Helmholtz equation, which is still linear, and the irrotational case is obtained when $c_1 = -d_1$.

### A.1.2 Case B: constant=$+r^2$

After dividing both sides of equation (A.3) by $Y^2$, it can be rewritten in the form

$$\frac{Y\,Y''' - Y'\,Y''}{Y^2} = +r^2\frac{Y\,Y'}{Y^2}, \tag{A.7}$$

which is equivalent to

$$\frac{\mathrm{d}}{\mathrm{d}y}\left(\frac{Y''}{Y}\right) = +r^2\frac{\mathrm{d}}{\mathrm{d}y}\log|Y|\,.$$

Upon integration, a second order differential equation is obtained

$$Y'' - r^2 Y\log|Y| + c_1 Y = 0, \tag{A.8}$$

where $c_1$ is again an arbitrary constant. Multiplying (A.8) by $Y'$ and integrating with respect to $y$, it follows

$$Y'^{\,2} + \left(c_1 + \frac{r^2}{2}\right) Y^{\,2} - Y^2\log|Y| = c_2\,, \tag{A.9}$$

where $c_2$ is another arbitrary constant. Making

$$\tilde{c}_1 = \exp\left[-\tfrac{1}{r^2}\left(c_1 + \tfrac{r^2}{2}\right)\right],$$
$$\tilde{c}_2 = c_2\,\tilde{c}_1^2\,/\,r^2,$$

as well as introducing the variables

$$\tilde{y} = r\,y \qquad \text{and} \qquad \tilde{Y} = \tilde{c}_1\,Y,$$

equation (A.9) reduces to a single family of trajectories given by

$$\tilde{Y}'^{\,2} - \tilde{Y}^2\log|Y| = \tilde{c}_2\,. \tag{A.10}$$

In the phase plane, there are three singular points — one center and two saddle points — and the trajectories associated with equation (A.10) are shown in figure (A.1). The following conclusions can be drawn about the nature of the solution:

1. for negative values of $\tilde{c}_2$, the solutions are unbounded, not periodic even functions;
2. for values of $\tilde{c}_2$ strictly between 0 and 0.1839 (=1/(2e)), all solutions are periodic with zero mean;

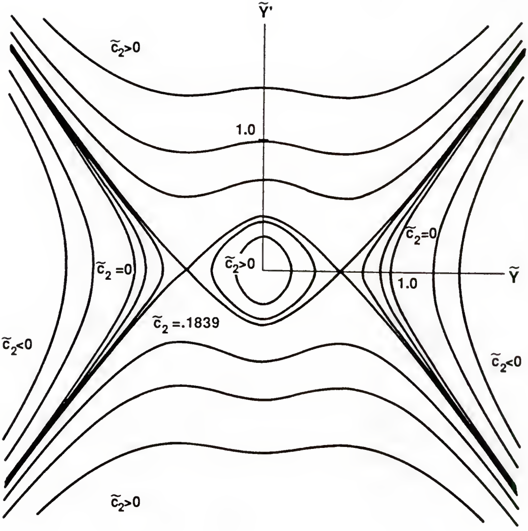

Figure A.1: Phase plane trajectories: Case B

3. for $\tilde{c}_2$ equal to 0.1839, there are three possible solutions (and their respective symmetric values);

4. for values of $\tilde{c}_2$ greater than 0.1839, the solutions are unbounded, not periodic odd functions.

As in Case A, it is valid to assume different values for the arbitrary constant in (A.8) for $X$ and $Z$, and the vorticity distribution will be given as

$$\omega \;=\; -\nabla^2\psi \;=\; (c_1 + d_1)\psi \;-\; r^2\psi\log|\psi|\,. \tag{A.11}$$

### A.1.3 Case C: constant=$-r^2$

Similar derivations as in Case B are valid, and the results can be written just changing appropriate signs. Therefore, the trajectories in the phase plane are defined by the family of equations

$$\tilde{Y}'^{\,2} \;+\; \tilde{Y}^2\log|Y| \;=\; \tilde{c}_2\,. \tag{A.12}$$

This change in sign however implies a totally different picture of the phase plane as can be seen in figure (A.2). The solutions in this case will always be periodic, but some distinction must be made for different values of $\tilde{c}_2$:

1. for $\tilde{c}_2$ strictly between -0.1839 and zero, the solutions have a positive mean value;

2. if $\tilde{c}_2$ equals zero, the solution is $\exp-(y^2/4)$;

3. for $\tilde{c}_2$ positive, the solutions have zero mean and six inflection points in one period – when $\tilde{Y} = 0$ and $\pm 1/\sqrt{e}$.

The vorticity distribution will be given as

$$\omega \;=\; -\nabla^2\psi \;=\; (c_1 + d_1)\psi \;+\; r^2\psi\log|\psi|\,. \tag{A.13}$$

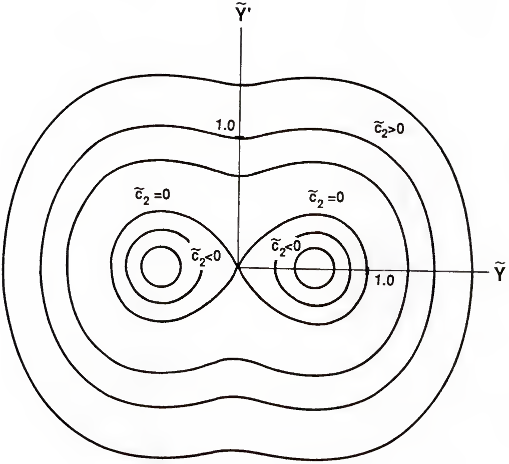

Figure A.2: Phase plane trajectories: Case C

## A.2 Application to the present theory

Regarding the formulation of the present wave theory, the solutions corresponding to Case C will be used. The stream function is formed by the product of a function of the horizontal variable and a function of the vertical variable. The horizontal dependency will be given by the trajectories with negative value of the parameter $\tilde{c}_2$, whereas the vertical dependency will be given by the trajectories with positive value of the parameter $\tilde{c}_2$.

# APPENDIX B
# NUMERICAL COMPUTATION OF lcc- AND lsc- FUNCTIONS FROM PHASE PLANE TRAJECTORIES

Both equations (A.10) and (A.12) have the same general form

$$Y'^2 + g(Y) = \tilde{c}, \tag{B.1}$$

and only periodic solutions are to be studied. Because the phase plane trajectory is a closed path, let $Y_1$ be the largest root of $g(Y) = \tilde{c}$. When this equation has more than one root, $Y_0$ will be chosen as its smallest, positive root. It is possible then to integrate (B.1) as

$$\frac{\mathrm{d}Y}{\sqrt{\tilde{c} - g(Y)}} = \mathrm{d}y \qquad \Rightarrow \qquad y - y_* = \int_{Y_*}^{Y} \frac{\mathrm{d}S}{\sqrt{\tilde{c} - g(S)}}. \tag{B.2}$$

Through this procedure, the independent variable is obtained as the result of the numerical integration of the right-hand side of (B.2). Since values of $Y$ have to be specified for carrying out the integration, actually the inverse function $Y^{-1}$ is first obtained.

As Y approaches $Y_1$ ( or $Y_0$ ), the integrand in (B.2) becomes singular. However, as long as $g'(Y_1)$ does not vanish,

$$\frac{1}{\sqrt{\tilde{c} - g(Y)}} \sim \frac{1}{\sqrt{|Y - Y_1|}},$$

which is integrable. As a matter of fact, since

$$g(Y) = \pm Y^2 \log|Y| \qquad \Rightarrow \qquad g'(Y) = \pm 2\,Y \log|Y| \pm Y,$$

where the +/- sign correspond to Cases B/C, respectively, in Appendix A. Hence, for $Y_1$ different from $1/\sqrt{e}$, $g'(Y_1)$ is not zero, and the integral in (B.2) is well defined.

Introducing a new variable of integration in (B.2) $u = s/Y_1$,

$$y = \int_{U_*}^{U} \frac{du}{\sqrt{\pm u^2 \log u \pm (u^2 - 1) \log Y_1}}, \qquad U = \frac{Y}{Y_1}. \tag{B.3}$$

Assigning values for U from 0.1 to 0.95, two methods were attempted for numerical integration of (B.3): trapezoid rule and Simpson's rule. The number of intervals was gradually increased until two successive values were equal to six digits. The functions *lsc*−, and *lcc*− are plotted in figures (3.3)-(3.2).

As $U$ approaches 1.0, a very large number of partitions becomes necessary. Either another numerical scheme should be used or some analytical transformation should be made in order to eliminate the singularity. The following numerical approaches were tried:

1. divide the interval [0,U] in several sub-intervals, applying Simpson's rule at each one, with different number of partitions for each sub-interval;
2. analytical approximation of the integral;
3. Gaussian quadrature.

The first method above still presented a difficult problem if the complete integral (i.e. for U=1.0) needed to be computed. Observing then that the singularity at U equal to 1.0 is of order $(u - 1)^{-1/2}$, it is possible to factor out this term, rewriting equation (B.3) as

$$y = \int_{U_*}^{U} \frac{1}{\sqrt{1-u}} \phi_\pm(u)\, du, \tag{B.4}$$

where

$$\phi_\pm(u) = \frac{1}{\sqrt{\pm \dfrac{u^2 \log u}{1-u} \mp (1+u) \log Y_1}}.$$

Because both limits at $u = 0$ and $u = 1$ exist for $\phi_\pm$,

$$\lim_{u \to 0} \phi_\pm(u) = (\mp \log Y_1)^{-\frac{1}{2}}$$

and

$$\lim_{u \to 0} \phi_{\pm}(u) = \lim_{u \to 0} \left( \frac{-1}{\pm 2u \log u \pm u \pm 2u \log Y_1} \right)^{\frac{1}{2}} = (\mp 2 \log Y_1 \mp 1)^{-\frac{1}{2}}$$

it follows that $\phi_+$ and $\phi_-$ are continuous functions in the interval $[0, 1]$. Therefore equation (B.4) can be integrated by parts to yield

$$y = \frac{2}{\sqrt{\mp \log Y_1}} - 2 \frac{\sqrt{1 - U}}{\sqrt{\pm \frac{U^2 \log U}{1-U} \mp (1 + U) \log Y_1}} + 2 \int_{U_*}^{U} \sqrt{1 - u} \frac{d\phi_{\pm}}{du} \, du. \quad \text{(B.5)}$$

Although the integrand in (B.5) is algebraically harder to compute, there should be no problem in carrying out the numerical integration up to $U = 1$ since the function is continuous. It turns out though, for values of $U \ll 1$, the number of steps necessary to achieve the same accuracy as Simpson's rule is much higher.

On the other hand, there are quadrature formulas appropriate for integrals of the type

$$I = \int \frac{1}{\sqrt{1 - x}} f(x) \, dx.$$

A very extensive review of such formulas is presented by Stroud and Secrest (1966), who also present the corresponding tables of constants in quadruple precision.

For numerical efficiency, it seems more reasonable that a combination of these methods be used depending on the limit of integration being considered. For the present study, a cutoff value was adopted of ±0.05 from the singularity. Within the region where the function is analytical, Simpson's rule is used for integrating (B.3) with the number of partitions equal to 100; within ±0.05 and ±0.0001, Simpson's rule is used for integrating (B.5) with the number of partitions equal to 1,000. For computing the complete integral, Gauss-Chebyshev quadrature is used with 20 partitions of the interval.

Table (B.1) gives the period $\lambda$, the extreme values $X_0$ and $X_1$, and the average value $\overline{X}$ of the function lcc- for different values of the parameter $\gamma_2$.

Table B.1: Computed parameters for $X(x;\gamma_2)$.

| $\gamma_2$ | $\lambda$ | $X_0$ | $X_1$ | $\overline{X}$ | $\Delta X/\overline{X}$ |
|---|---|---|---|---|---|
| -.005 | 8.192390 | 0.039306 | 0.994962 | 0.435690 | 2.193433 |
| -.007 | 8.019834 | 0.048016 | 0.992925 | 0.445880 | 2.119203 |
| -.010 | 7.834567 | 0.059537 | 0.989846 | 0.457544 | 2.033268 |
| -.030 | 7.251944 | 0.118629 | 0.968524 | 0.500429 | 1.698332 |
| -.050 | 6.977499 | 0.167198 | 0.945618 | 0.524945 | 1.482860 |
| -.070 | 6.796672 | 0.212638 | 0.920748 | 0.543111 | 1.303803 |
| -.090 | 6.661993 | 0.257591 | 0.893356 | 0.557881 | 1.139607 |
| -.100 | 6.605697 | 0.280461 | 0.878459 | 0.564407 | 1.059516 |
| -.110 | 6.554881 | 0.303899 | 0.862564 | 0.570490 | 0.979271 |
| -.120 | 6.508593 | 0.328178 | 0.845455 | 0.576198 | 0.897742 |
| -.130 | 6.466109 | 0.353645 | 0.826830 | 0.581584 | 0.813614 |
| -.140 | 6.426865 | 0.380791 | 0.806235 | 0.586689 | 0.725162 |
| -.150 | 6.390415 | 0.410381 | 0.782939 | 0.591547 | 0.629802 |
| -.160 | 6.356397 | 0.443781 | 0.755599 | 0.596186 | 0.523022 |
| -.170 | 6.324516 | 0.484034 | 0.721194 | 0.600628 | 0.394853 |
| -.180 | 6.294527 | 0.542599 | 0.668284 | 0.604895 | 0.207780 |

# APPENDIX C
# MINIMIZATION PROCEDURE

In the minimization of the objective function given by equation (3.16),

$$\mathcal{O} = \frac{2}{\lambda}\int_0^{\lambda/2} \left(Q-\overline{Q}\right)^2 \,\mathrm{d}x + l_1\left(|\eta(0) - \eta(\lambda/2)| - 1\right) + l_2\frac{2}{\lambda}\int_0^{\lambda/2} \eta \,\mathrm{d}x \qquad \text{(C.1)}$$

it becomes necessary to determine the derivatives of the Bernoulli constant, Q, with respect to the several parameters. The expressions used in the numerical model were actually approximations since the derivatives of the functions $lcc-$ and $lsc-$ with respect to their parameters were not computed. Hence, letting

$$Q = \eta + \frac{\alpha\epsilon^2}{\delta_1^2}\left(\gamma_2 Z^2 + \delta_2 X^2\right), \quad \text{at } z = \epsilon(1+\alpha\eta), \qquad \text{(C.2)}$$

it follows:

$$\frac{\partial Q}{\partial \gamma_2} = -\frac{1}{\alpha\epsilon}\frac{1}{X_1^2+2\gamma_2}\frac{Z}{Z'} + \frac{1}{2}\frac{\alpha\epsilon^2}{\delta_1^2}\frac{X_1^2 Z^2 + 2\delta_2 X^2}{X_1^2 + 2\gamma_2} \qquad \text{(C.3)}$$

$$\frac{\partial Q}{\partial \delta_1} = \frac{1}{\delta_1\alpha\epsilon}\frac{Z}{Z'} - \frac{\alpha\epsilon^2\delta_2}{\delta_1^3}X^2 \qquad \text{(C.4)}$$

$$\frac{\partial Q}{\partial \delta_2} = -\frac{1}{\alpha\epsilon}\frac{1}{Z_1^2+2\delta_2}\frac{Z}{Z'} + \frac{1}{2}\frac{\alpha\epsilon^2}{\delta_1^2}X^2 \qquad \text{(C.5)}$$

$$\frac{\partial Q}{\partial \epsilon} = \frac{\alpha\epsilon}{\delta_1^2}\left(\gamma_2 Z^2 + \delta_2 X^2\right) - \frac{1+\alpha\eta}{\alpha\epsilon} \qquad \text{(C.6)}$$

$$\frac{\partial Q}{\partial \psi_\eta} = \frac{\delta_1}{\alpha\epsilon X Z'}\left[1 + \frac{\alpha^2\epsilon^3\gamma_2}{\delta_1^2}\right]. \qquad \text{(C.7)}$$

The derivatives of the free surface with respect to the same parameters were computed as:

$$\frac{\partial \eta}{\partial \delta_1} = \frac{1}{\delta_1\alpha\epsilon}\frac{Z}{Z'} \qquad \text{(C.8)}$$

$$\frac{\partial \eta}{\partial \gamma_2} = -\frac{1}{\alpha\epsilon}\frac{1}{X_1^2+2\gamma_2}\frac{Z}{Z'} \qquad \text{(C.9)}$$

$$\frac{\partial \eta}{\partial \delta_2} = -\frac{1}{\alpha \epsilon} \frac{1}{Z_1^2 + 2\delta_2} \frac{Z}{Z'} \tag{C.10}$$

$$\frac{\partial \eta}{\partial \epsilon} = -\frac{1 + \alpha \eta}{\alpha \epsilon} \tag{C.11}$$

$$\frac{\partial \eta}{\partial \psi_\eta} = \frac{\delta_1}{\alpha \epsilon X Z'} . \tag{C.12}$$

As in section 3.2, let $\xi_i^n$ denote any of the varying parameters at iteration $n$. Expanding the system represented by equation (3.18), a symmetric matrix is obtained. In truly nonlinear least squares method, that matrix is always positive definite, which allows the use of special algorithms. In the present case however that property is not valid. The matrix can be represented as

$$\begin{pmatrix} \mathrm{E}_{11} & \mathrm{E}_{12} & \cdots & \mathrm{F}^1_{10} & \mathrm{F}^2_{10} \\ \mathrm{E}_{21} & \mathrm{E}_{22} & \cdots & \mathrm{F}^1_{20} & \mathrm{F}^2_{20} \\ \cdots & \cdots & \cdots & \cdots & \cdots \\ \mathrm{F}^1_{10} & \mathrm{F}^1_{20} & \cdots & 0 & 0 \\ \mathrm{F}^2_{10} & \mathrm{F}^2_{20} & \cdots & 0 & 0 \end{pmatrix} \begin{pmatrix} \Delta\xi_1 \\ \Delta\xi_2 \\ \cdots \\ \Delta l_1 \\ \Delta l_2 \end{pmatrix} = \begin{pmatrix} \mathrm{E}_{10} + l_1 \mathrm{F}^1_{10} + l_2 \mathrm{F}^2_{10} \\ \mathrm{E}_{20} + l_1 \mathrm{F}^1_{20} + l_2 \mathrm{F}^2_{20} \\ \cdots \\ \mathrm{F}^1_{00} \\ \mathrm{F}^2_{00} \end{pmatrix}$$

where a subscript $j$ represents derivative with respect to the parameter $\xi_j$,

$$\mathrm{E}_{ij} = \overline{\frac{\partial Q}{\partial \xi_i} \frac{\partial Q}{\partial \xi_j}} - \overline{\frac{\partial Q}{\partial \xi_i}}\, \overline{\frac{\partial Q}{\partial \xi_j}},$$

and $\mathrm{F}^1$ and $\mathrm{F}^2$ are the constraints imposed on the free surface elevation, respectively,

$$\mathrm{F}^1 = |\eta(0) - \eta(\lambda/2)| - 1$$

$$\mathrm{F}^2 = \frac{2}{\lambda} \int_0^{\lambda/2} \eta \, dx.$$

The subscript 0 indicates no derivative is taken.

At each iteration, this system is solved using the subroutine LEQT1F from the IMSL package.

# BIBLIOGRAPHY

Benjamin, T. B. (1962). "The solitary wave on a stream with an arbitrary distribution of vorticity," J. Fluid Mechanics, v. 12, pp. 97-116.

Chaplin, J. R. (1980). "Developments of a stream-function wave theory," Coastal Engineering, v.3, pp. 179-205.

Conte, S. D. and C. de Boor (1980). Elementary Numerical Analysis. An Algorithmic Approach, 3rd. edition, McGraw-Hill, New York.

Dalrymple, R. A. (1973). "Water Wave Models and Wave Forces with Shear Currents," COE Technical Report 20, University of Florida.

Dalrymple, R. A. (1977). "A numerical model for periodic finite amplitude waves on a rotational fluid," J. Computational Physics, v.24, 1, pp. 29-42.

Dalrymple, R. A. and J. C. Cox (1976). "Symmetric finite-amplitude rotational water waves," J. Physical Oceanography, v. 6, 6, pp. 847-852.

Dean, R. G. (1965). "Stream function representation of nonlinear ocean waves," J. Geophysical Research, v. 70, 18, pp. 4561- 4572

Dubreil-Jacotin, M. L. (1934). "Sur la détermination rigoureuse des ondes permanentes périodiques d'ampleur finie," Journal de Mathématiques, v. 13, 3, pp. 217-291.

Helmholtz, H. v. (1858). "Über Integrale der hydrodynamischen Gleichungen, welche den Wirbelbewegungen entsprechen," Crelle, v. 55, pp. 25-55; translated by Tait, Phil. Mag., 4, v. 33, pp. 485.

Hunt, J. N. (1955). "Gravity waves in flowing water," Proc. Royal Society London, Ser. A, v. 231, pp. 496-504.

Kinsman, B. (1984). Wind Waves, Dover, New York.

Lamb, H. (1932). Hydrodynamics, 6th. edition, Dover, New York.

Lambrakos, K. (1981). "Extended velocity potential wave kinematics," J. Waterway, Port, Coastal and Ocean Engineering, ASCE, v. 107, WW3, pp. 159-174.

Peregrine, D. H. (1976). "Interaction of water waves and currents," Adv. Applied Mechanics, v. 16, pp. 10-117.

Peregrine, D. H. and I. G. Jonsson (1983). "Interaction of waves and currents," Report MR 83-6, US Army, Coastal Engineering Research Center, Fort Belvoir.

Peregrine, D. H., I. G. Jonsson and C. Galvin (1983). "Annotated bibliography on wave-current interaction," Report MR 83-7, US Army, Coastal Engineering Research Center, Fort Belvoir.

Rienecker, M. M. and J. D. Fenton (1981). "A Fourier approximation method for steady water waves," J. Fluid Mechanics, v. 104, pp. 119-137.

Stroud, A. H. and D. Secrest (1966). Gaussian Quadrature Formulas, Prentice-Hall, Englewood Cliffs, NJ.

Taylor, G. I. (1955). "The action of a surface current used as a breakwater," Proc. Royal Society London, Ser. A, v. 231, pp. 466-478.

Yih, C. S. (1955). "On a method of generating three- dimensional potential flows from two-dimensional ones," Quart. Applied Mathematics, v. 13, 3, pp. 320-322.

Yih, C. S. (1972). "Surface waves in flowing water," J. Fluid Mechanics, v. 51, pp. 209-220.

# BIOGRAPHICAL SKETCH

Mr. Claudio Neves was born February 24, 1955, in Rio de Janeiro, Brazil. In 1973 he started his studies at the Federal University of Rio de Janeiro, pursuing simultaneously a major in civil engineering (B.S., 1977), and in mathematics (B.S.,1978). His interest in coastal engineering began during the senior year in engineering, when a graduate program in ocean engineering at the same university was formed, the first of its kind in Brazil, from which he obtained a M.Sc. degree in 1979.

I certify that I have read this study and that in my opinion it conforms to acceptable standards of scholarly presentation and is fully adequate, in scope and quality, as a dissertation for the degree of Doctor of Philosophy.

Robert G. Dean

Robert G. Dean, Chairman
Graduate Research Professor of
Engineering Sciences and Coastal
and Oceanographic Engineering

I certify that I have read this study and that in my opinion it conforms to acceptable standards of scholarly presentation and is fully adequate, in scope and quality, as a dissertation for the degree of Doctor of Philosophy.

Thomas T. Bowman

Thomas T. Bowman
Associate Professor of Mathematics

I certify that I have read this study and that in my opinion it conforms to acceptable standards of scholarly presentation and is fully adequate, in scope and quality, as a dissertation for the degree of Doctor of Philosophy.

Joseph L. Hammack

Joseph L. Hammack
Professor of Engineering Sciences

I certify that I have read this study and that in my opinion it conforms to acceptable standards of scholarly presentation and is fully adequate, in scope and quality, as a dissertation for the degree of Doctor of Philosophy.

James T. Kirby

James T. Kirby
Assistant Professor of Coastal and
Oceanographic Engineering

I certify that I have read this study and that in my opinion it conforms to acceptable standards of scholarly presentation and is fully adequate, in scope and quality, as a dissertation for the degree of Doctor of Philosophy.

Hsiang Wang
Professor of Coastal and
Oceanographic Engineering

This dissertation was submitted to the Graduate Faculty of the College of Engineering and to the Graduate School and was accepted as partial fulfillment of the requirements for the degree of Doctor of Philosophy.

December 1987

Hubert A. Bevis
Dean, College of Engineering

Dean, Graduate School